Cardiovascular Research

Heart failure leads to altered beta2-adrenoceptor/cAMP dynamics in the sarcolemmal phospholemman/Na,K ATPase microdomain

--Manuscript Draft--

Manuscript Number:	CVR-2017-375R1
Full Title:	Heart failure leads to altered beta2-adrenoceptor/cAMP dynamics in the sarcolemmal phospholemman/Na,K ATPase microdomain
Short Title:	Phospholemman cAMP microdomain
Article Type:	Original Article
Keywords:	cAMP, phospholemman, phosphodiestarase, FRET, heart failure
Corresponding Author:	Viacheslav Nikolaev University Medical Center Hamburg-Eppendorf Hamburg, GERMANY
Corresponding Author Secondary Information:	
Corresponding Author's Institution:	University Medical Center Hamburg-Eppendorf
Corresponding Author's Secondary Institution:	
First Author:	Zeynep Bastug-Özel
First Author Secondary Information:	
Order of Authors:	Zeynep Bastug-Özel
	Peter T Wright
	Axel E Kraft
	Davor Pavlovic
	Jacqueline Howie
	Alexander Froese
	William Fuller
	Julia Gorelik
	Michael J Shattock
	Viacheslav Nikolaev
Order of Authors Secondary Information:	
Abstract:	Aims: Cyclic adenosine monophosphate (cAMP) regulates cardiac excitation-contraction coupling by acting in microdomains associated with sarcolemmal ion channels. However, local real time cAMP dynamics in such microdomains has not been visualized before. We sought to directly monitor cAMP in a microdomain formed around sodium-potassium ATPase (NKA) in healthy and failing cardiomyocytes and to better understand alterations of cAMP compartmentation in heart failure. Methods and Results: A novel Förster resonance energy transfer (FRET)-based biosensor termed PLM-Epac1 was developed by fusing a highly sensitive cAMP sensor Epac1-camps to the C-terminus of phospholemman (PLM). Live cell imaging in PLM-Epac1 and Epac1-camps expressing adult rat ventricular myocytes revealed extensive regulation of local cAMP levels by beta2-adrenoceptors (beta2-ARs) and co-localized (by immunofluorescence) pools of phosphodiesterase (PDE) type 3. In chronic heart failure following myocardial infarction, dramatic reduction of the microdomain-specific beta2-AR/cAMP signals and beta2-AR dependent PLM phosphorylation was accompanied by a pronounced loss of local PDE3 and an increase in PDE2 effects.

Powered by Editorial Manager® and ProduXion Manager® from Aries Systems Corporation

	Conclusions: NKA/PLM complex forms a distinct cAMP microdomain which is directly regulated by beta2-ARs and is under predominant control by PDE3. In heart failure, local changes in PDE repertoire result in blunted beta2-AR signaling to cAMP in the vicinity of PLM.

Powered by Editorial Manager® and ProduXion Manager® from Aries Systems Corporation

Abstract

Heart failure leads to altered β_2-adrenoceptor/cAMP dynamics in the sarcolemmal phospholemman/Na,K ATPase microdomain

Bastug-Özel et al.

***Aims*:** Cyclic adenosine monophosphate (cAMP) regulates cardiac excitation-contraction coupling by acting in microdomains associated with sarcolemmal ion channels. However, local real time cAMP dynamics in such microdomains has not been visualized before. We sought to directly monitor cAMP in a microdomain formed around sodium-potassium ATPase (NKA) in healthy and failing cardiomyocytes and to better understand alterations of cAMP compartmentation in heart failure.

***Methods and Results*:** A novel Förster resonance energy transfer (FRET)-based biosensor termed PLM-Epac1 was developed by fusing a highly sensitive cAMP sensor Epac1-camps to the C-terminus of phospholemman (PLM). Live cell imaging in PLM-Epac1 and Epac1-camps expressing adult rat ventricular myocytes revealed extensive regulation of local cAMP levels by β_2-adrenoceptors (β_2-ARs) and co-localized (by immunofluorescence) pools of phosphodiesterase (PDE) type 3. In chronic heart failure following myocardial infarction, dramatic reduction of the microdomain-specific β_2-AR/cAMP signals and β_2-AR dependent PLM phosphorylation was accompanied by a pronounced loss of local PDE3 and an increase in PDE2 effects.

***Conclusions*:** NKA/PLM complex forms a distinct cAMP microdomain which is directly regulated by β_2-ARs and is under predominant control by PDE3. In heart failure, local changes in PDE repertoire result in blunted β_2-AR signaling to cAMP in the vicinity of PLM.

Cover Letter/Declaration

Institute of Experimental Cardiovascular Research
Prof. Dr. Viacheslav Nikolaev
Director

Center for Experimental Medicine

Martinistraße 52
20246 Hamburg
Gebäude W 23, Raum 2.04
Phone: +49 (0) 40 7410-51391
Fax: +49 (0) 40 7410-40180
v.nikolaev@uke.de
www.uke.de

Universitätsklinikum Hamburg-Eppendorf | Martinistraße 52 | 20246 Hamburg
Institut für Experimentelle Herz- Kreislaufforschung

Dr. Karin Sipido
Editor-in-Chief
Cardiovascular Research

Hamburg, 22.11.2017

Revised Manuscript submission CVR 2017-375

Dear Dr. Sipido, Dear Karin,

We would like to submit an extensively revised version of our manuscript entitled "**Heart failure leads to altered β_2-adrenoceptor/cAMP dynamics in the sarcolemmal phospholemman/Na,K ATPase microdomain**" for your kind consideration as an *Original Article* in *Cardiovascular Research*.

In doing the revision, we gave our best to experimentally address all major and minor concerns raised by the Reviewers as detailed in the point-by-point response in a separate Rebuttal Letter. We believe that our study should be of high interest to the broad readership of *Cardiovascular Research* since it provides important new data on therapeutically relevant cAMP microdomain signaling and mechanistic insights into its alterations in heart failure. We hope that in this revised form, our manuscript is now suitable for publication.

All authors agree with the contents of the manuscript and its submission. We would be thankful if you could exclude Manuela Zaccolo (due to direct competition) and Rodolphe Fischmeister (due to close collaboration) from the review process.

Many thanks for your kind consideration.

Sincerely yours,



Slava (Nikolaev)

Reviewer #1:

Bastug et al. investigates changes in the putative microdomains of PLM-NKA-β2AR in the setting of heart failure by utilizing a FRET-based PLM-Epac1-camps cAMP biosensor. Normal adult rat ventricular myocytes (ARVMs) are isolated from both normal and infarct-induced failing rat hearts. Immunofluorescence and immunoprecipitation was used to assess PLM|NKA|PDE co-localizations, and live-cell FRET imaging was used to assess PLM-NKA association (reflecting, cAMP generation), thus support for a PLM-NKA-β2AR-PDE microdomain. Manuscript was well written. Results were supportive of a PLM-NKA-β2AR-PDE3A microdomain that was disrupted upon heart failure. In general, the experimental approach and results were convincing, and conclusions were appropriate. However, I do have some major and minor concerns as follows:

Major concerns:

- The authors state that the PLM, NKA, beta2ARs and PDE3A are largely localized in the t-tubules, and t-tubules are significantly disrupted in heart failure, as the authors referred to in the Discussion. The authors have included confocal image analyses, and state that PLM-Epac1 sensor shown confocal images and indicate that it is largely in the t-tubules and co-localizes with PLM|NKA|PDE. The authors further state in the Discussion that 2ARs are also exclusively located it the t-tubules, and so generate localized cAMP responses that do not propagate into the deep cytosol containing SR and contractile proteins.

- First, to decisively discern t-tubule localization, z-stack confocal images should be acquired for both normal and heart failure myocytes. This is rather important, as culturing myocytes more than 24hrs typically leads to some remodeling - including the beginnings of t-tubules loss - that needs to be assessed.

We thank the Reviewer for raising this important points. Though localization on endogenous PLM has been attributed to t-tubules in previous literature (see also response to Reviewer 2, Comment 3), this has not previously been done for our sensor. Following the Reviewer's advice, we have now stained normal and failing PLM-Epac1 sensor expressing myocytes with caveolin 3 antibody and performed z-stack confocal analysis. To the best of our knowledge cav3 alone with di-8-ANEPPS live stain (which is challenging to perform together with the FRET sensor due to spectral overlap) is the most suitable marker to stain for t-tubuli. These confocal data are now presented in the **new Supplementary Figures 6 and 7**. Indeed, PLM-Epac1 sensor co-localized quite well with t-tubules in both healthy and MI cells.

- Second, I am at odds with the authors inferring that localization in the t-tubules does not allow for propagation into the deep cytosol contain SR and contractile proteins? Is this actually not the purpose of t-tubules?? It certainly is for calcium signaling. Please clarify your statement/meaning.

Indeed, in case of calcium signals, t-tubules are essential for CICR bringing L-type channels and ryanodine receptors into close proximity. For cAMP this might be a bit more complicated. Indeed, using FRET imaging combines with scanning ion conductance microscopy in the cited Science 2010 reference, we could see that close proximity of SR to T-

tubules can restrict cAMP diffusion, especially from beta2AR by two means: firstly, local pools of PKA located in the cleft between t-tubules and SR can buffer some cAMP; secondly, this PKA can activate local PDE4 which degrades cAMP. We have clarified it a bit more extensively now in the discussion, see **page 11, 3rd paragraph.**

- Third, if heart failure leads to the loss of t-tubules, thus disrupting the PLM-NKA-beta2AR microdomain and thereof loss of the PDE3 selectivity, then would not the loss of t-tubules essentially account for this?

Sure, it could. This is a realistic possibility, which is also one of the major reasons for beta2AR redistribution. We have added this into the discussion, see at the top of **page 13 (first paragraph):**

"The drop of β_2-AR/cAMP signal in the vicinity of NKA/PLM could be, at least in part, a result of β_2-AR redistribution from T-tubules to detubulated membrane areas which has been previously described for failing cardiomyocytes isolated the same MI-induced disease model[24]. Potentially, detubulation could promote also PDE3 redistribution, thereby affecting local cAMP degradation.**"**

- Fourth, the authors have insinuated that beta2ARs are "redistributed from t-tubules"…but my hunch is that this is more a direct effect of t-tubule loss…and correspondingly, perhaps beta2AR loss. The authors should check for a downward change in beta2ARs levels/expression (i.e., qPCR and more importantly Western blots) in their heart failure model.

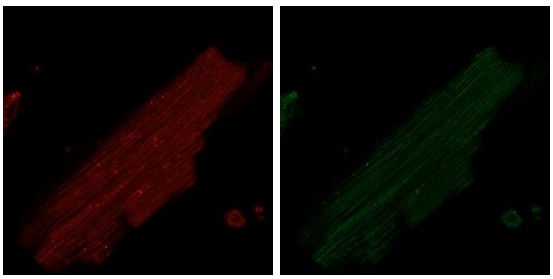
We thank the Reviewer for this helpful suggestion. We have done new experiments and looked at beta1AR and beta2AR levels by Western blot (which is also a bit challenging bearing in mind that the specificity of antibodies is rather limited). We could see clear reduction of beta1AR expression which is characteristic for chronic heart failure model. However, beta2AR expression was virtually unchanged which is in line with some previous studies on the role and expression of beta2AR in heart failure. We have added these data into **new Supplementary Fig. 4A**. See also other panels of the figure and the response to Reviewer 3, comment 2: there we did some additional blots and qPCR for other components of the cAMP pathway.

Minor Concerns:

- Fixing cells with ethanol can result in translocation from plasmalemma to cytosol/nucleus. Perhaps if not already done so, a comparison of fixation with paraformaldehyde compared against that with ethanol would be important, as microdomain location is key focus here?

We thank the Reviewer for this suggestion. Following this point, we have stained PFA fixed cells for Supplementary Fig. 1 C,D and all new IF images performed during revision (see

above and below). There were no obvious differences in respect to PLM and NKA localization. For PDE3 we had to stay with ethanol fixation since this antibody (we have tried several commercial and self-made PDE3 antibodies available) does not properly work after PFA fixation – here is an example of such a staining:



Autofluorescence **PDE3**

Reviewer #2:

The Authors are expert in the use of the Epac-camps reagent, and employed a PLM-coupled sensor to analyze its proximity to other signaling molecules in cultured primary adult rat cardiomyocytes, expressing the sensor by an adenovirus ostensibly with a CMV promoter, although many important details of this aspect of the experimental system were referenced elseware. The data shows unsurprising sensitivity of the PLM sensor to increased levels of cAMP, but the relevance of this to NKA is questionable, as discussed below.

1.

Fig. 1

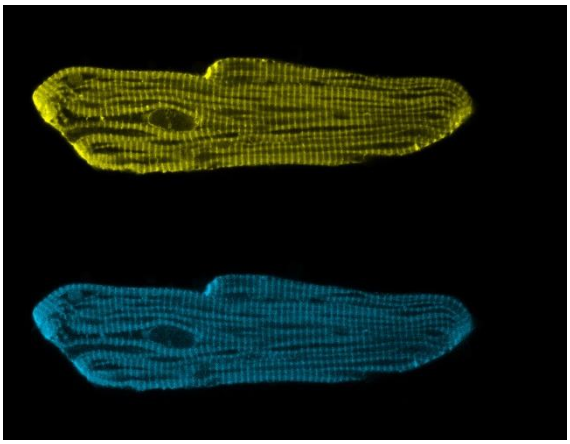
Both the Control and PLM-Epac are aligned along T-tubules. If the Control sensor is "cytosolic" as the Authors claim, then it must be binding to an ER/SR protein, as the fluorescent pattern is indistinguishable from classic SR patterns, and highly similar to that of PLM-Epac except for its completeness. The pattern observed for PLM-Epac is also classic for a protein of the biosynthetic/secretory pathway, and shows a pattern consistent with early protein synthesis, where rough ER compartments around the nucleus are packed with newly made PLM. The punctate SR pattern shows the early stages of Epac-PLM trafficking through the cell, almost certainly in ER/SR, where the cell is trying to get it to the outer plasma membrane. Only a minor portion of the protein appears to make it to the mature sarcolemmal form. Again, the large amount of perinuclear protein is typical of a protein that has overwhelmed the biosynthetic pathway. There is no specific evidence that the protein has matured and trafficked to the plasma membrane, which would appear as an intense fluorescence around the cell periphery. The observed effect of Iso on FRET, within the white box shown, is also a measure of SR puncta in or around junctional SR puncta. This early population of transverse SR tubules of adenovirally overexpressed (i.e. newly-made) proteins in adult cardiomyocytes appears to be part of normal intracellular trafficking (see e.g. Sleiman et al., J. Mol. Cell. Cardiol., 81, 34 (2015).

We would like to thank the Reviewer for raising this important point. Indeed, adenovrial overexpression of PLM-Epac1 construct may generate artefacts which should be carefully controled for. An earlier study by Lansbery et al AJP 290 C1275-86 (2006) has suggested that over-expressed PLM is retained in the ER in the absence of NKA to associate with an traffic to the plasma membrane. Hence the 'overexpressed' sensor PLM is indeed retained in an intracellular compartment, and only PLM associated with the pump is probably 'making it' out to the cell surface.

To make sure that we are measuring the specific response of the mature sensor at the membrane, we have changed our strategy to select the region where we calculate FRET ratios. Instead of using the previously shown white box (in our old data, we actually rather unsystematicly used variety of regions – whole cell, white box, just the outer membrane region), we now systematically re-analyzed all the PLM-Epac1 measurements using a membrane region shown in the Figure 1C which excluded any perinuclear and other dotted artefacts found in the cells enterior. In this case, the shapes and magnitudes of FRET changes were quite similar to previous values, so this overall did not lead to changes in conclusions obtained from our experiments. We have carefully updated FRET traces and dot plots for the PLM-Epac1 sensor in Figures 1, 2, 3 and 4. Figure 5 was not chaged since we already used a

membrane region for analysis of these data before. Interestinly, when we tried to detect FRET signals in a perinuclear region with strong overexpression, there was on obvious change in signal upon ISO stimulation, as shown in the **new Figure 1C**. This suggests that these overexpression areas might indeed contain immature sensor protein which is not capable of reporting dynamics changes in cAMP, and therefore should not interfere with the overall signal. We hope that by systematically using a membrane region, we have now provided a better more reliable way to analyse our FRET data. We have now commented on these changes made in Text, at the **bottom of page 7.**

As for the cytosolic sensor Epac1-camps, we are pretty sure this this protein is very well soluble and should not be targeted to SR. Many staining ot fluorescent pattern in adult myocytes look striated in confocal, although one would not expect them to localize. We noticed it for a sobulble cytosolic cAMP biosensor (Nikolaev et al. Circ Res 2006; 99:1084-1091 , Figure 2D). We have also tried another «cytosolic» sensor AKAR-NES (A-kinase activity reported, developed by J Zhang and used in myocytes e.g. by Haj Slimane et al Cardiovasc Res. 2014 Apr 1;102(1):97-106.) it shows just a simalar pattern as our Epac1-camps:



2.

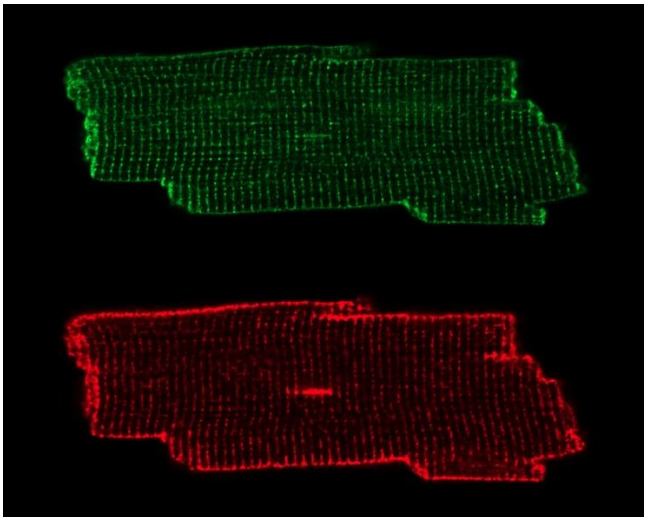
Supplementary Fig. 2 data is confusing, and authors do not account for all of the protein bands. If the 75 kDa band is solely due to the PLM-sensor, why do the authors not dilute the samples to allow a comparison between the native PLM (17 kDa) and the overexpressed PLM protein sensor. There are a lot of alternative MW species. Authors need to explain how such a mammoth amount of PLM cannot overwhelm their detection system. The concentration of the protein in the early parts of the secretory pathway could be expected to provide substantial ambiguity to the localization of cAMP production.

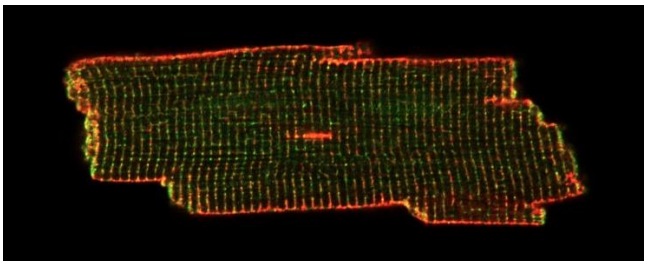
Many thanks for bringing up this important point. Our feeling is that due to adenoviral overexpression, a large numbers of lower MW species are present on the blots because the immature protein has overwhelmed the secretory pathway and could be partially degraded. These lower MW species are largely non-functional FRET wise, as shown above, since they do not contain both fluorophores linked to cAMP binding domains and PLM. We have commented on these issues in the **Discussion on page 11, second paragraph**. For the most crucial Co-IP experiments in the Supplem. Fig 2, we have also provide a low exposure blot image.

3.

In the Discussion (p. 10), the Authors state that "Based on biochemical evidence and co-localization experiments, PLM-Epac1 sensor was properly targeted to the microdomain of interest and retained functional properties of unmodified PLM in terms of physical association with α1-subunits and inhibition of NKA function (see Supplementary Figures 1 and 2). Similar to endogenous PLM, it localized largely in the transverse (T) tubules where functional β2-AR are also detected24". The reference here to their own work on beta-2 receptor localization, but localization of native PLM to T-tubules is not supported by any published data, to our knowledge. Indeed, the authors did not show localization data for native PLM. These facts, unfortunately, undermine the basic construct of the experimental system as declared by the authors in this statement. Together with the gross overexpression of the PLM sensor, and its obvious concentration in the early parts of the secretory pathway, the possibility is raised that the FRET responses do not have the desired physiological relevance that the data and finding rely upon.

Indeed, although there were some previous reports suggesting that PLM and overexpressed co-localizes with NKA at the T-tubules (see e.g. the immunofluorescence in Silverman et al Cardiovascular Research 65, 93-103 (Figure 7) or Figure 6 in Himes RD et al. Biochemistry. 2016;55:6196-6204 – WGA co-stain), bona fide immunofluorescence localization for our study (for endogenous PLM and PLM-Epac1) to T-tubules was missing. To improve this, we have stained PLM-Epac1 transfected healthy and failing myocytes with caveolin 3 antibody, which is one of the most suitable markers to stain for t-tubuli in fixed cells. These confocal data confirming clear t-tubular localization of PLM sensor are now presented in the **new Supplementary Figures 6 and 7**. See also our response to Reviewer 1, Comment 1. PLM-Epac1 co-localized nicely with a1-subunit of NKA, as did the endogenous PLM – see Supplem Fig 1C/D. Therefore, there is no doubt that endogenous PLM is localize to T-tubuli. We also did this direct co-localization of endogenous PLM (green) with cav3 (red) which we did not included into the manuscript:





4. ***There is explicit mention of GFP in the schematic structure of the PLM sensor construct, so the anti-GFP data was confusing.***

Sorry about that. The reason for this confusion is that we were using anti-GFP antibody to detect CFP and YFP mutants which are present in our sensor(s). We have added this explanation into the legend of Supplementary Fig. 1

Reviewer #3:

In this manuscript, the authors used a novel FRET-based cAMP-sensor to monitor the microdomain formation between NKA and cAMP proteins in both healthy and post-MI heart failure (HF) rat ventricular myocytes. Multiple pharmaceutical inhibitors were used to dissect the contribution of different isoforms of PDE in the regulation of beta-adrenergic signaling in NKA microdomains in control and HF. The topic is significant and the approach is novel. But I have several concerns listed below:

1) This study used a novel cAMP sensor PLM-Epac1 and overexpressed the sensor in control and HF myocytes to assess the association-dissociation balance of cAMP and NKA. However, additional evidence is required to verify whether overexpressed PLM-Epac1 can compete with WT-PLM for binding with NKA and whether this sensor dissociates from NKA when the c-terminus of PLM is phosphorylated like WT-PLM. If the sensor does not have similar dissociation kinetics with NKA as compared to that of WT-PLM, then expressed exogenous PLM-Epac1 sensor may alter the function of NKA.

We thank the Reviewer for this point. It has been shown in the previous literature that PLM does not dissociate from NKA on phosphorylation (which is somewhat in contrast to PLB/SERCA complex). See for example -Bossuyt J et alJ Biol Chem. 2009;284:26749-57. This study used FRET constructs (PLM and NKA fused to CFP and YFP) and classical co-IP to monitor conformational changes in the PLM/NKA complex and associated of both protein upon PKA-mediated phosphorylation. In this case the FRET relationship is changed, but the proteins still co-immunoprecipitate with each other when PLM is phosphorylated.
Pavlović D et al FASEB J. 2007;21:1539-46 have also previously demonstrated that both S68 phosphorylated and unphosphorylated PLM associate with NKA alpha1 subunit by coimmunprecipitation.
We believe that when expressed in myocytes PLM-Epac1 sensor (at least its fraction which is trafficked to plasma membrane) associates with endogenous NKA early after protein synthesis. Our co-immunoprecipitation data (Supplem Fig 2) at least indirectly indicate endogenous PLM is competed-out by the PLM-Epac sensor in this case.

2) The authors assessed beta-adrenergic signaling in a HF rat model. The cAMP-NKA relationship in HF vs control was presented as normalized YFP/CFP ratio. It is known that beta-adrenergic signaling strength alters in different stages of HF. In the early stages of diminished cardiac function, beta-adrenergic signaling increases in an attempt to compensate for decreased cardiac function, eventually, the chronic catecholamine stimulation leads to the downregulation of beta-ARs which in turn leads to waning beta-adrenergic signaling. Here, the status of the beta-adrenergic signaling components (i.e. beta-AR expression& function (binding affinity), adenylyl cyclase, PKA, etc) was not assessed. Most importantly, the effect of local cAMP on PLM phosphorylation and NKA activity should be assessed in both HF and b-AR stimulated samples to strengthen the results of PLM-Epac1 sensor data in this manuscript.

We thank the Reviewer for raising this important point. We have performed additional experiments to look at the expression of beta1AR, beta2AR, PKA RI and RII subunits, adenylyl cyclases 5 and 6 in out heart failure models –please, see the **new Supplem Fig. 4**. We could

see that beta1AR was downregulated (as expected for our HF model), while the expression of beta2AR, PKA R subunits and AC5/6 were not significantly changed. We also analyzed beta2AR/PKA-mediated PLM phosphorylation in heathy and failing myocytes by immunoblot in Figure 6.

3) The authors used the FRET signals from PLM-Epac1 sensor to probe the local cAMP variation under various conditions: beta-1 AR challenging, beta-2 AR challenging, HF, various PDE inhibitor treatment etc. Immunohistology staining data would be a way to assess the spatial correlations of PLM-Epac1 and NKA under different challenge conditions. In addition, the selectivity of CGP and ICI for b1-AR and b2-AR need to be addressed.

We thank the Reviewer for this helpful suggestion! In the revised manuscript we provide a new **Supplementary Figure 5** which shows immunostaining to analyze co-localization of PLM-Epac1 sensor with NKA a-subunit under various stimulated conditions or in HF as suggested. Analysis of co-localization coefficient indicates that there is not significant change in co-localization in any of these conditions. To address the selectivity of CGP and ICI for beta1 and beta2-AR, we added a sentence into the text **on page 12, second paragraph** which refers to our published experiments in beta1/beta2-AR KO mice which support the selectivity of these blockers at concentrations used. Initially, these concentrations have been established based on bona fide pharmacological literature such as Hoffmann C. et al. Naunyn Schmiedebergs Arch Pharmacol. 2004369(2):151-9.

4) It is known and the authors acknowledged that PKC can also phosphorylate the c-terminus of PLM in addition to the PKA actions. Yet the authors did not address the contribution of PKC that might complicate the contribution of the PLM-Epac1 signals observed in these studies (for instance, they could contribute to the localization of overexpressed sensor, or the signal read-out of the sensor).

Many thanks for this important suggestion. To check the effect of PKC on our FRET readout, we stimulated PLM-Epac1 expressing cells with PMA which did not lead to any detectable change in FRET. We included these data into the text on **page 7 (at the bottom).** Also, as suggested by the Reviewer we checked by immunostaining if PMA treatment would affect PLM-Epac1 colocalization with NKA a-subunit – which did not- please, see the **new Supplementary Figure 5.**

5) A number of pharmacological reagents were used in the studies (i.e. 100nM isopreterenol for beta-AR challenge; 100nM isopreterenol plus 100nM of beta1-AR blocker CGP20712A as beta2-AR agonist; 100nM BAY 60-7550 for PDE2 selective inhibitor; 10uM cilostamide as PDE3 inhibitor; 10uM rolipram for PDE4 inhibitor; 100uM IBMX as unselective PDE inhibitor). Either valid citations or experimental results for the specific concentration and treatment time frame should be presented to verify the potency and specificity of the pharmacological reagents used in the studies.

In addition to commenting on CGP and ICI specificity, as indicated under point 3 above, we have included some further citations (at the **bottom of page 8**) which use the same

concentrations of the PDE inhibitors BAY, cilostamide and rolipram in PDE activity assays and FRET assays to selectively block PDE2, 3 or 4, respectively.

6) There are a few occasions that an abbreviation was used before definition. The experiments involving Epac1-camps weren't thoroughly introduced in the methods. Also, this manuscript used many pharmaceutical reagents to inhibit different isoforms of PDEs, details of the inhibitors should be introduced to the readers.

Thank you for this helpful comment. We carefully check the text and introduced abbreviation on their first use. PDE inhibitor were also better introduced, see also point 5 above. We have also now thoroughly introduced Epac1-camps and its principle in the first paragraph of the Results section (see the **bottom of page 6**):

Epac1-camps is a cytosolic cAMP sensor which contains a cyclic nucleotide binding domain derived from Epac1 which is sandwiched between two green fluorescent protein (GFP) mutants, namely enhanced cyan (CFP) and yellow fluorescent protein (YFP). In the absence of cAMP, CFP and YFP are located in close proximity, generating a high degree of FRET signal. Binding of cAMP to Epac1 domain leads to a conformational change in the biosensor molecules which brings both fluorophores far apart, decreasing the FRET signal[27].

7) There are some immunoblot analyses of low gel quality, such as Fig. Sup1, Sup2.

Thank you very much for raising this important point. We did our best to improve quality of Western Blots or select films with lower expose where possible. We could not find any better blots for Suppl Fig. 1. However, we provided a shorter exposure of the most crucial Co-IP blot in the **Suppl Fig. 2B**.

Handling Editor

The author should address convincingly the concerns about potential methodological artifacts arising from overexpression and distinguish protein trafficking from co-localization. The confounding changes with cell culture need to be carefully considered.
We have addressed both major issues doing new experiments exactly as instructed by Reviewers – see responses above.

Editorial comments:

- Please specify which method was used to sacrifice the MI animals.
Added into Methods section: "sacrificed 16 weeks after MI by cervical dislocation in isoflurane anaesthesia"

- Which data sets were analyzed using Mann-Whitney tests?
Sorry for the generic error (not properly mentioning the stat tests, i.e. Mann-Whitney). In Fig. 3C (BAY groups) and in Supplementary Fig. 5B, Mann-Whitney test has been used since data sets were not normally distributed. This has been corrected in the figure legend.

- To allow better evaluation of the Western blot data in figure 6, all 4 conditions should be presented on a single blot. Please also provide the Western blot for total PLM protein and normalize towards this.
We did our best to provide immunoblots which use total PLM as a loading control. We reloaded our old samples used for Figure 6 and even made many new samples and used various stripping protocols. However, it was not possible for us to reprobe the same membrane after stripping off P-PLM antibody for total PLM in a reliable manner. Since our aim was to qualitatively assess beta2AR-induced PLM phosphorylation in healthy and HF cells, we did not intend to compare PLM expression in healthy vs HF (which has been done before e.g by J Bossuyt and D Bers, e.g. in Circ Res 2005) on the same blot.

Finally, please make sure kDa values are added for all blots.
Added for all blots

- Scale bars should be provided for all images.
Added in all confocal images.

- Please consider reorganizing the main manuscript to highlight some of the results and methods currently in the supplement. The journal can allow up to 7000 words in the main text and 7 main figures with an additional half-page schematic highlighting the major findings.
We carefully considered reorganizing the main manuscript. Since the number of figures was already 7, we did not move any supplementary figures into the main ms. However, we moved some methods (sensor construction) into the main text, since shown in the main ms. Methods describing results shown in Supplementary Figure were left in Supplement. Some

new discussion has been added into the text, so that the word number has now increased.

Checklist

- Highlight in the manuscript all changes that have been made;
All changes are underlined.

- ***Mention in the cover letter all changes in the title and / or authors and repeat all necessary declarations as stated in our instructions to authors;***
Done

- Use the manuscript number CVR-XXXX in the running head of every page.
CVR-2017-375 added on every page

Heart failure leads to altered β_2-adrenoceptor/cAMP dynamics in the sarcolemmal phospholemman/Na,K ATPase microdomain

Bastug et al. Phospholemman cAMP microdomain

Zeynep Bastug-Özel,[1,2] PhD, Peter T. Wright,[3] PhD, Axel E. Kraft[4,5], Mr, Davor Pavlovic,[6] PhD, Jacqueline Howie,[7] PhD, Alexander Froese,[4,5] PhD, William Fuller,[7] PhD, Julia Gorelik,[3] PhD, Michael J. Shattock,[2*] PhD, and Viacheslav O. Nikolaev,[4,5*] PhD

[1]Clinic of Cardiology and Heart Research Center, University Medical Center Göttingen, Göttingen, Germany;

[2]Cardiovascular Division, King's College London, London, UK;

[3]National Heart and Lung Institute, Imperial College London, London, UK;

[4]Institute of Experimental Cardiovascular Research, University Medical Center Hamburg-Eppendorf, Hamburg, Germany;

[5]German Center for Cardiovascular Research (DZHK), Partner site Hamburg/Kiel/Lübeck, Germany

[6]Institute of Cardiovascular Sciences, University of Birmingham, Birmingham, UK;

[7]Division of Cardiovascular and Diabetes Medicine, University of Dundee, Dundee, UK

*M.J.S. and V.O.N. share the senior authorship

Address for correspondence:

Prof. Dr. Viacheslav O. Nikolaev
Institute of Experimental Cardiovascular Research
University Medical Center Hamburg-Eppendorf
Martinistr. 52
D-20246 Hamburg, Germany
Phone: +49-40-7410-51391; Fax: +49-40-7410-40180
E-mail: v.nikolaev@uke.de

Abstract

***Aims*:** Cyclic adenosine monophosphate (cAMP) regulates cardiac excitation-contraction coupling by acting in microdomains associated with sarcolemmal ion channels. However, local real time cAMP dynamics in such microdomains has not been visualized before. We sought to directly monitor cAMP in a microdomain formed around sodium-potassium ATPase (NKA) in healthy and failing cardiomyocytes and to better understand alterations of cAMP compartmentation in heart failure.

***Methods and Results*:** A novel Förster resonance energy transfer (FRET)-based biosensor termed PLM-Epac1 was developed by fusing a highly sensitive cAMP sensor Epac1-camps to the C-terminus of phospholemman (PLM). Live cell imaging in PLM-Epac1 and Epac1-camps expressing adult rat ventricular myocytes revealed extensive regulation of local cAMP levels by β_2-adrenoceptors (β_2-ARs) and co-localized (by immunofluorescence) pools of phosphodiesterase (PDE) type 3. In chronic heart failure following myocardial infarction, dramatic reduction of the microdomain-specific β_2-AR/cAMP signals and β_2-AR dependent PLM phosphorylation was accompanied by a pronounced loss of local PDE3 and an increase in PDE2 effects.

***Conclusions*:** NKA/PLM complex forms a distinct cAMP microdomain which is directly regulated by β_2-ARs and is under predominant control by PDE3. In heart failure, local changes in PDE repertoire result in blunted β_2-AR signaling to cAMP in the vicinity of PLM.

Key words: cAMP, phospholemman, phosphodiestarase, FRET, heart failure

Introduction

3',5'-cyclic adenosine monosphosphate (cAMP) as an ubiquitous second messenger regulates cardiomyocyte function by acting in discrete subcellular microdomains. Such microdomains are formed for example around ion channels participating in excitation-contraction (EC) coupling and involve a set of differentially localized receptors, cAMP-dependent protein kinase (PKA) with its anchoring proteins, and cAMP hydrolyzing enzymes phosphodiesterases (PDEs) which are crucial for spatial confinement of cyclic nucleotide gradients in cells[1, 2]. Functionally distinct cAMP microdomains have previously been described in caveolin-rich membrane structures[3], various subsarcolemmal locations[4] and around sarcoplasmic reticulum calcium ATPase[5]. However, local cAMP dynamics in any microdomain directly associated with a sarcolemmal ion channel involved in EC coupling and its changes in cardiac disease have not been studied before.

An important cAMP microdomain might be associated with the sodium-potassium ATPase (NKA), a sarcolemmal pump which, as the predominant Na^+ efflux mechanism in cardiomyocytes, maintains the transmembrane Na^+ gradient. This gradient is essential not only for a variety of Na-dependent membrane transporters but also for the rapid upstroke of action potential upon depolarization[6, 7]. Subsequent elevation of intracellular Ca^{2+} triggers cell contraction followed by the diastolic Ca^{2+} extrusion via the sodium-calcium exchanger (NCX) in its forward mode which in turn is promoted by the transmembrane Na^+ gradient[8]. Therefore, NKA activity orchestrates calcium cycling and EC coupling. In heart failure, an increase in intracellular Na^+, in part due to a decline in NKA activity, dissipates this Na^+ gradient and hence contributes to altered Ca cycling, diastolic dysfunction, arrhythmias and changes in mitochondrial metabolism[9-12].

Phospholemman (PLM, also known as FXYD1) is a 72 amino acid transmembrane muscle cell protein[13-15] which forms a stable complex with NKA[16, 17]. The cytosolic C-terminus of PLM

bears at least three different phosphorylation sites, one of them Ser68 can be phosphorylated by the cAMP-dependent protein kinase (PKA) and protein kinase C[18-20]. PLM tonically inhibits NKA, and PLM phosphorylation by PKA leads, via a conformational change occurring without a dissociation, to an increase of NKA activity (its sodium affinity and transport kinetics), thereby lowering intracellular sodium load during increases in heart rate under β-adrenoceptor (β-AR) stimulation[21]. Conversely, hypo-phosphorylation of PLM, as occurs in heart failure, exacerbates contractile dysfunction, increases Na^+ overload and promotes myocardial remodeling[22]. Despite the importance of PLM phosphorylation in both normal and pathophysiology, local cAMP dynamics in this critical microdomain has not been directly investigated.

Here, we developed a novel targeted Förster resonance energy transfer (FRET)-based cAMP biosensor to monitor real time cAMP dynamics in the vicinity of the NKA/PLM complex. FRET measurements uncovered tight regulation of this microdomain by the β_2-AR/cAMP/PKA and local pools of PDE3, which was lost in heart failure. These data provide a molecular basis for better understanding of disease-associated local signalling changes and may help develop new therapies to prevent sodium overload in heart failure.

Methods

Detailed methods section is available in the *Supplementary Material*.

Chemicals. BAY 60-7550 was from Santa Cruz. Cilostamide, rolipram, (-) isoproterenol (ISO), forskolin, CGP20712A and ICI118551 were purchased from Sigma. 3-isobutyl-1-methylxanthine (IBMX) was from Applichem. All other chemicals were from Sigma, unless stated otherwise.

Sensor construction. Full-length canine PLM sequence lacking the stop codon was fused via a flexible liner encoding the KRSRAQASNSAVDGTPVATG amino acid sequence to the N-terminus of Epac1-camps (Ref. 27). The adenovirus generation is performed using the Gateway® Cloning system (Life Technologies) and in accordance with the manufacturer´s instructions.

FRET-based cAMP measurements in cardiomyocytes. Rat were anesthetized by isoflurane inhalation and sacrificed by cervical dislocation. Adult rat ventricular myocytes (ARVMs) were isolated by enzymatic Langendorff perfusion, transduced for 48 h with Epac1-camps or PLM-Epac1 adenoviruses and subjected to FRET measurements as described[23,24]. Imaging was performed at room temperature in the buffer containing in mmol/L: NaCl 144, KCl 5.4, $MgCl_2$ 1, $CaCl_2$ 1, HEPES 10, pH=7.3. Compounds were diluted in the same buffer and applied onto cells cumulatively if not stated otherwise.

Myocardial infarction (MI) chronic heart failure model. All animal experiments were performed in accordance with Guide for the Care and Use of Laboratory Animals published by the U.S. National Institutes of Health under assurance number A5634-01. All surgical procedures and perioperative management conformed to the UK Animals (Scientific Procedures) Act 1986 and were approved by the Animal Welfare and Ethical Review Body (AWERB) Committee of Imperial College London. Adult male Sprague-Dawley rats (250–300

g) underwent proximal coronary ligation to induce MI under isoflurane anaesthesia as previously described[24, 25]. Righting reflex was used to monitor the adequacy of anaesthesia. For analgesia, metamizole (300 mg/kg/day in drinking water 3 days prior and 7 days after surgery) and buprenorphine (0.05 mg/kg subcutaneously, 30 min prior to and every 8 h during 7 days after surgery) were used. Rats were functionally characterized by echocardiography and sacrificed 16 weeks after MI by cervical dislocation in isoflurane anaesthesia for cardiomyocyte isolation. Echocardiographic and functional parameters of the rats used in this study have been previously described[26].

Statistics. Normal distribution was tested by the Kolmogorov-Smirnov test. Differences were analyzed using OriginPro8.6 (OriginLab, Northampton) or R software (R Foundation for Statistical Computing) and one-way ANOVA or Mann-Whitney tests, followed by Bonferroni's post-hoc test, as appropriate. When several cells isolated from the same animal were considered, mixed ANOVA followed by Wald χ^2-test was used. Data are presented as means±SE from the indicated number of experiments (animals and cells) per condition.

Results

Generation and characterization of a novel targeted PLM-Epac1 biosensor

To enable real time measurements of cAMP directly in the NKA/PLM microdomain, we sought to develop a targeted version of the highly sensitive FRET biosensor Epac1-camps[27]. Epac1-camps is a cytosolic cAMP sensor which contains a cyclic nucleotide binding domain derived from Epac1 which is sandwiched between two green fluorescent protein (GFP) mutants, namely enhanced cyan (CFP) and yellow fluorescent protein (YFP). In absence of cAMP, CFP and YFP are located in close proximity, generating a high degree of FRET signal. Binding of cAMP to Epac1 domain leads to a conformational change in the biosensor

molecules which brings both fluorophores far apart, decreasing the FRET signal[27]. Based on a previously developed functional PLM-YFP construct containing a flexible 20 amino acid linker between canine PLM and YFP sequence[28], we fused our cAMP sensor sequence in a similar way to the PLM C-terminus (**Figure 1A**). When introduced into adult rat ventricular myocytes by adenoviral gene transfer (at the multiplicity of infection MOI 300), this targeted biosensor was found in the surface membrane and co-localized well with the endogenous NKA α_1-subunits, similar to native PLM (**Supplementary Figure 1A-D**). It could also inhibit NKA activity in transfected cells and be co-immunoprecipitated with endogenous cardiomyocyte NKA α_1-subunits in both directions (**Supplementary Figure 2A-C**), confirming PLM functionality inside the PLM-Epac1 biosensor. Fluorescence in PLM-Epac1 expressing cardiomyocytes showed membrane localization in transverse (T)-tubules and outer sarcolemma) with a clear striated pattern and some perinuclear overexpression (most likely related to the biosynthetic pathway and intracellular trafficking machinery), areas that were excluded from image data analysis (**Figure 1B,C**). Stimulation of cells with the β-adrenergic agonist isoproterenol (ISO) led to a rapid decrease in YFP and a concomitant increase in CFP fluorescence in the membrane cell region, indicative of a decrease in YFP/CFP ratio and an increase of local cAMP levels (**Figure 1C**). Interestingly, no detectable change of FRET signal could be recorded in the perinuclear region with strong overexpression, suggesting that the sensor molecules might be still immature in this compartment and should not be affecting functionally relevant biosensor recordings. Also, no detectable change of FRET signal in the membrane regions could be observed in cells stimulated with saturating concentrations (10 µmol/L) of protein kinase C activator Phorbol 12-myristate 13-acetate (change in FRET 0.09±0.11 %, followed by a positive control 10 µmol/L forskolin plus 100 µmol/L IBMX which caused 9.9±0.6 % decrease of FRET ratio, number of animals/cells 4/10).

FRET imaging shows considerable β_2-adreneceptor/cAMP signals in the vicinity of PLM

Next, we performed FRET measurements under selective stimulation of β_1- and β_2-adrenoceptors (ARs), the major cAMP stimulating adrenergic receptor subtypes expressed in cardiomyocytes. Selective β_1-AR stimulation performed as previously established[3, 5, 24, 29] led to comparable cAMP signals in PLM-Epac1 and Epac1-camps expressing myocytes, suggesting similar degree of local cAMP increase as in the bulk cytosol (**Figure 2A,B**). In sharp contrast, β_2-AR/cAMP responses were nearly doubled in the PLM/NKA microdomain, as compared to the cytosol (**Figure 2C-E**), suggesting close functional association of this receptor subtype with PLM. We directly compared the affinities of both biosensors to cAMP and their sensitivities to ISO stimulation in intact ARVMs, using a previously established protocol[23]. Interestingly, the affinity of PLM-Epac1 was slightly lower than that of Epac1-camps (**Supplementary Figure 3A**), suggesting that the actual defence in β_2-AR/cAMP between bulk cytosol and PLM/NKA microdomain might be even greater. Using these sensor calibration data, we recalculated FRET values into absolute cAMP concentrations which were 0.73 ± 0.04 and 2.95 ± 0.41 µM for global (cytosolic) vs. local β_2-AR stimulated cAMP, respectively. Interestingly, the potencies derived from concentration-response dependencies for ISO measured with both sensors were comparable (**Supplementary Figure 3B**). This suggests that β-adrenergic stimulation in general leads to higher cAMP levels at NKA/PLM as compared to the bulk cytosol, which is compatible with the idea of privileged receptor – microdomain communication previously observed also for the phospholamban microdomain[5].

Role of PDEs in shaping cAMP signals in the NKA/PLM microdomain

To understand how cAMP dynamics is regulated at the local level, we next studied the effects of various PDE inhibitors at basal state and after β_1-AR- or β_2-AR-selective receptor stimulations in healthy cells. The concentrations of PDE inhibitors used have been previously established in FRET and PDE activity assays to be selective for the respective PDE

families[3,5]. In the absence of prestimulation with β-AR ligands, there were no significant differences found in the effects of PDE3 and PDE4 selective inhibitors between bulk cytosol and the NKA/PLM microdomain. However, the local contribution of PDE2 was significantly higher in the vicinity of PLM (**Figure 3**). After β_1-AR stimulation, all three PDE family inhibitors showed no significant differences in FRET responses between the two sensors (**Figure 4C**). In sharp contrast, the contribution of PDE3 was strikingly much more pronounced in the NKA/PLM microdomain after β_2-AR prestimulation (**Figure 4A,B,D**). These FRET data correspond to 1.2 ± 0.1 and 31.0 ± 12.2 µM of global (cytosolic) vs. local cAMP, respectively, after cilostamide application in presence of β_2-AR stimulation. These data indicate that local cAMP dynamics at PLM is tightly controlled by PDE2 at basal state and by PDE3 after β_2-AR stimulation, while PDE4 effects are present but not significantly different in both locations.

Heart failure blunts local β_2-AR control and alters PDE2/PDE3 balance in the NKA/PLM microdomain

Since cardiac disease has been associated with changes in cAMP signaling, we next investigated how the NKA/PLM microdomain is affected in the rat model of chronic heart failure induced by myocardial infarction. 16 weeks after MI when the chronic failing phenotype has been established, ARVMs were isolated and transduced with either cytosolic Epac1-camps or with targeted PLM-Epac1 biosensor. At this stage of disease, as expected, β_1-AR levels were downregulated whereas the expression of β_2-AR, regulatory PKA subunits and adenylyl cyclases 5 and 6 were not significantly changed (**Supplementary Figure 4**). Importantly, heart failure did not lead to detectable changes of PLM-Epac1 sensor co-localization with endogenous NKA α_1-subunit, nor was this co-localization affected by various pharmacological treatments used in our study (**Supplementary Figure 5**). Heart

failure also did not visibly affect the intracellular localization of the sensor which could be found in T-tubular and membrane regions expressing caveolin 3 (**Supplementary Figure 6,7**) Strikingly, heart failure led to a loss of the local β_2-AR/cAMP signal compartmentation, leading to FRET responses which were indistinguishable from those measured in the cytosol (**Figure 5A-E**). These FRET values correspond to 0.8 ± 0.1 and 1.9 ± 0.2 µM of cytosolic vs. local β_2-AR stimulated cAMP, respectively. Interestingly, while there were no major disease-driven changes in PDE effects detected in the cytosol (**Supplementary Figure 8**), measurements with PLM-Epac1 sensor in failing cells after β_2-AR stimulation revealed a significant increase in local PDE2 inhibitor effects accompanied by a decrease in microdomain-specific PDE3 effects (**Figure 5A-D,F**). Finally, using immunofluorescence, we detected a clear co-localization of PDE3 with PLM which was significantly reduced in heart failure (**Supplementary Figure 9**). Importantly, as expected from the FRET data (see Figures 2E and 5E), β_2-AR selective stimulation led to a clear phosphorylation of PLM at the Ser68, and this effect was abolished in failing cells (**Figure 6**).

Discussion

Despite a clear evidence that cAMP modulates cardiac excitation-contraction coupling by acting in microdomains associated with sarcolemmal ion channels, local compartmentalized cAMP dynamics in their close proximity has not been analyzed before. In this study, we directly monitored local cAMP dynamics in the vicinity of NKA by creating a novel PLM-targeted FRET biosensor and using it in healthy and failing adult rat ventricular myocytes.

Based on biochemical evidence and co-localization experiments, PLM-Epac1 sensor was properly targeted to the microdomain of interest and retained functional properties of unmodified PLM in terms of physical association with α_1-subunits and inhibition of NKA function (see Supplementary Figures 1 and 2). Similar to endogenous PLM, it localized largely in T-tubules and outer membrane regions expressing caveolin 3 (Supplementary Figures 6 and 7). However, adenoviral overexpression of the sensor led to a perinuclear overexpression artefact and several lower molecular weight band of immunoblots (see Supplementary Figure 2) which may result from immature and/or degraded sensor protein. Importantly, there was no detectable change in FRET upon stimulation of cAMP production when recorded from perinuclear overexpression areas (see Figure 1C), suggesting that these irrelevant protein species do not interfere with specific cAMP recordings.

In our previous study, using scanning ion conductance microscopy in combination with FRET-based cAMP recordings, we could detect β_2-AR/cAMP signals originating from functional receptors exclusively located in T-tubules of healthy ARVMs[24]. This T-tubular localization of the β_2-AR leads to local cAMP confinement by PKA-dependent buffering and activation of PDE4. In contrast, β_1-AR as the predominant β-AR subtype was evenly distributed across the sarcolemma. β_1-AR modulation leads to changes in cAMP signals in both cytosolic and sarcolemmal membrane microdomains, to strong contractile responses and promotes cardiac remodelling. In contrast, functional β_2-ARs are exclusively located in T-

tubules, thereby generating highly localized cAMP responses which do not significantly diffuse into the deep cytosol containing sarcoplasmic reticulum and contractile proteins but may protect from pathological remodelling[24, 30]. Therefore, one may expect a functional interaction of β_2-AR with NKA/PLM.

Indeed, our FRET-based analysis revealed much stronger β_2-AR/cAMP responses in the NKA/PLM microdomain, as compared to the bulk cytosol (see Figure 2). This suggests an important functional coupling of β_2-AR with this microdomain, which, in addition to much more abundant β_1-AR stimulated cAMP, might critically regulate NKA function. To selectively activate β_1- and β_2-AR subtypes, we used a combination.of the unselective β-adrenergic agonist ISO together with β_1- and β_2-AR subtype-selective antagonists CGP20712A and ICI118551 which we established to be selective at the respective concentrations using β_1- and β_2-AR knockout mice[24].

It is tempting to speculate that β_2-AR could also play a cardioprotective role by inducing a local pool of cAMP which leads to phosphorylation of PLM and protection from Ca^{2+} overload. However, in chronic heart failure, this cAMP microdomain becomes disrupted (see Figure 5E) which may limit the potentially beneficial effects of β_2-AR. Previously, Juel and colleagues showed that β_2-AR activation modulates NKA activity in human skeletal muscle[31], although PLM phosphorylation was not examined in this study. Two other reports[32, 33] showed that pharmacological β_2-AR agonists (terbutaline and formoterol) both increased PLM Ser68 phosphorylation in human skeletal muscle. Here, we report for the first time that β_2-AR signaling modulates local cAMP gradients around the NKA/PLM microdomain, leading to PKA-mediated PLM phosphorylation in cardiac myocytes which is changed in disease. Our FRET data go in line with immunoblot analysis which shows that selective β_2-AR stimulation leads to an increase of PLM phosphorylation, and that this effect is clearly abolished in heart failure (see Figure 6). The drop of β_2-AR/cAMP signal in the vicinity of

NKA/PLM could be, at least in part, a result of β_2-AR redistribution from T-tubules to detubulated membrane areas which has been previously described for failing cardiomyocytes isolated the same MI-induced disease model[24]. Potentially, detubulation could promote also PDE3 redistribution, thereby affecting local cAMP degradation.

Equally important could be changes in PDE composition of the NKA/PLM microdomain detected in this study. By analyzing the effects of the selective inhibitors for the major cardiomyocyte cAMP hydrolyzing PDEs (2, 3 and 4), we found that the NKA/PLM microdomain is under stringent PDE2 dependent control at basal state, while after β_2-AR stimulation, PDE3 becomes dominant (see Figures 3 and 4). This is comparable with the data from adult mouse cardiomyocytes obtained using a targeted version of the Epac1-camps sensor localized in the caveolin-rich membrane microdomains including T-tubules (pmEpac)[3]. Using immunofluorescence, significant co-localization of PDE3A with endogenous PLM could be observed, with a clear reduction in heart failure (see Supplementary Figure 9). Likewise, functional effect of the PDE3 inhibitor cilostamide on cAMP levels in the NKA/PLM microdomain was dramatically reduced in failing cells (see Figure 5C,D,F). Instead, the local effect of PDE2 was significantly increased (see Figure 5A,B,F). This important PDE has been previously shown to be upregulated at the mRNA and protein level in various heart failure models[34], and seems to affect especially the local microdomain signalling (Figure 7), while no significant disease-driven alterations could be detected in the bulk cytosol (Supplementary Figure 8). Previously, using an early disease model of compensated cardiac hypertrophy induced by transverse aortic constriction in pmEpac expressing mice, we uncovered a PDE2 and PDE3 redistribution between β_1- and β_2-AR-associated caveolar and non-caveolar membrane microdomains. In this case, PDE3 as the predominant PDE family at the β_2-AR was substituted by PDE2, leading to changes in cGMP/cAMP cross-talk engaged by atrial natriuretic peptide receptors[3]. Obviously, a similar change in PDE repertoire in the NKA/PLM microdomain can be now detected also in a chronic rat heart failure model (see Figure 5). This change of the microdomain-specific PDE

composition should definitely affect the rates of cAMP hydrolysis resulting in a change of responsiveness to β_2-AR stimulation. The modulation of the local cAMP response by cGMP associated with atrial and brain natriuretic peptide signaling is unlikely to play a role in this decompensated late disease model because of the desensitization of their common NPR1 receptor which is typical for chronic heart failure[35].

In summary, we provide the first direct visualization of local cAMP signaling at a sarcolemmal cardiomyocyte ion channel regulated in a microdomain formed around the NKA/PLM complex. FRET based live cell imaging indicates tight regulation of this microdomain by the β_2-AR and local pools of PDE3 and its dramatic alteration in heart failure. This knowledge could provide a molecular basis for novel therapeutic strategies to prevent disease-associated sodium overload and impaired excitation-contraction coupling.

Acknowledgments

We thank Tobias Goldak and Karina Schlosser for ARVM isolation and technical assistance.

Conflict of Interest

None declared.

Funding

The work was supported by the Deutsche Forschungsgemeinschaft (IRTG1816 to V.O.N. and M.J.S.), Wellcome Trust (109604/Z/15/Z to D.P.), British Heart Foundation (RG/12/18/30088 to J.G.) and the Gertraud und Heinz-Rose Stiftung (to V.O.N.).

References

1. Perino A, Ghigo A, Scott JD, Hirsch E. Anchoring proteins as regulators of signaling pathways. *Circ Res* 2012;**111**:482-492.
2. Perera RK, Nikolaev VO. Compartmentation of cAMP signalling in cardiomyocytes in health and disease. *Acta Physiol (Oxf)* 2013;**207**:650-662.
3. Perera RK, Sprenger JU, Steinbrecher JH, Hubscher D, Lehnart SE, Abesser M, Schuh K, El-Armouche A, Nikolaev VO. Microdomain switch of cGMP-regulated phosphodiesterases leads to ANP-induced augmentation of beta-adrenoceptor-stimulated contractility in early cardiac hypertrophy. *Circ Res* 2015;**116**:1304-1311.
4. Rochais F, Vandecasteele G, Lefebvre F, Lugnier C, Lum H, Mazet JL, Cooper DM, Fischmeister R. Negative feedback exerted by cAMP-dependent protein kinase and cAMP phosphodiesterase on subsarcolemmal cAMP signals in intact cardiac myocytes: an in vivo study using adenovirus-mediated expression of CNG channels. *J Biol Chem* 2004;**279**:52095-52105.
5. Sprenger JU, Perera RK, Steinbrecher JH, Lehnart SE, Maier LS, Hasenfuss G, Nikolaev VO. In vivo model with targeted cAMP biosensor reveals changes in receptor-microdomain communication in cardiac disease. *Nat Commun* 2015;**6**:6965.
6. Skou JC. The influence of some cations on an adenosine triphosphatase from peripheral nerves. *Biochim Biophys Acta* 1957;**23**:394-401.
7. Blaustein MP. Sodium ions, calcium ions, blood pressure regulation, and hypertension: a reassessment and a hypothesis. *Am J Physiol* 1977;**232**:C165-173.
8. Bers DM, Despa S. Na+ transport in cardiac myocytes; Implications for excitation-contraction coupling. *IUBMB Life* 2009;**61**:215-221.
9. Pogwizd SM. Clinical potential of sodium-calcium exchanger inhibitors as antiarrhythmic agents. *Drugs* 2003;**63**:439-452.
10. Verdonck F, Volders PG, Vos MA, Sipido KR. Intracellular Na+ and altered Na+ transport mechanisms in cardiac hypertrophy and failure. *J Mol Cell Cardiol* 2003;**35**:5-25.
11. Pieske B, Maier LS, Piacentino V, 3rd, Weisser J, Hasenfuss G, Houser S. Rate dependence of [Na+]i and contractility in nonfailing and failing human myocardium. *Circulation* 2002;**106**:447-453.
12. Liu T, O'Rourke B. Enhancing mitochondrial Ca2+ uptake in myocytes from failing hearts restores energy supply and demand matching. *Circ Res* 2008;**103**:279-288.

13. Palmer CJ, Scott BT, Jones LR. Purification and complete sequence determination of the major plasma membrane substrate for cAMP-dependent protein kinase and protein kinase C in myocardium. *J Biol Chem* 1991;**266**:11126-11130.
14. Bogaev RC, Jia LG, Kobayashi YM, Palmer CJ, Mounsey JP, Moorman JR, Jones LR, Tucker AL. Gene structure and expression of phospholemman in mouse. *Gene* 2001;**271**:69-79.
15. Wetzel RK, Sweadner KJ. Phospholemman expression in extraglomerular mesangium and afferent arteriole of the juxtaglomerular apparatus. *Am J Physiol Renal Physiol* 2003;**285**:F121-129.
16. Crambert G, Fuzesi M, Garty H, Karlish S, Geering K. Phospholemman (FXYD1) associates with Na,K-ATPase and regulates its transport properties. *Proc Natl Acad Sci U S A* 2002;**99**:11476-11481.
17. Khafaga M, Bossuyt J, Mamikonian L, Li JC, Lee LL, Yarov-Yarovoy V, Despa S, Bers DM. Na(+)/K(+)-ATPase E960 and phospholemman F28 are critical for their functional interaction. *Proc Natl Acad Sci U S A* 2012;**109**:20756-20761.
18. Walaas SI, Czernik AJ, Olstad OK, Sletten K, Walaas O. Protein kinase C and cyclic AMP-dependent protein kinase phosphorylate phospholemman, an insulin and adrenaline-regulated membrane phosphoprotein, at specific sites in the carboxy terminal domain. *Biochem J* 1994;**304 (Pt 2)**:635-640.
19. Han F, Bossuyt J, Despa S, Tucker AL, Bers DM. Phospholemman phosphorylation mediates the protein kinase C-dependent effects on Na+/K+ pump function in cardiac myocytes. *Circ Res* 2006;**99**:1376-1383.
20. Fuller W, Howie J, McLatchie LM, Weber RJ, Hastie CJ, Burness K, Pavlovic D, Shattock MJ. FXYD1 phosphorylation in vitro and in adult rat cardiac myocytes: threonine 69 is a novel substrate for protein kinase C. *Am J Physiol Cell Physiol* 2009;**296**:C1346-1355.
21. Despa S, Tucker AL, Bers DM. Phospholemman-mediated activation of Na/K-ATPase limits [Na]i and inotropic state during beta-adrenergic stimulation in mouse ventricular myocytes. *Circulation* 2008;**117**:1849-1855.
22. Boguslavskyi A, Pavlovic D, Aughton K, Clark JE, Howie J, Fuller W, Shattock MJ. Cardiac hypertrophy in mice expressing unphosphorylatable phospholemman. *Cardiovasc Res* 2014;**104**:72-82.
23. Börner S, Schwede F, Schlipp A, Berisha F, Calebiro D, Lohse MJ, Nikolaev VO. FRET measurements of intracellular cAMP concentrations and cAMP analog permeability in intact cells. *Nat Protoc* 2011;**6**:427-438.

24. Nikolaev VO, Moshkov A, Lyon AR, Miragoli M, Novak P, Paur H, Lohse MJ, Korchev YE, Harding SE, Gorelik J. Beta2-adrenergic receptor redistribution in heart failure changes cAMP compartmentation. *Science* 2010;**327**:1653-1657.
25. Lyon AR, MacLeod KT, Zhang Y, Garcia E, Kanda GK, Lab MJ, Korchev YE, Harding SE, Gorelik J. Loss of T-tubules and other changes to surface topography in ventricular myocytes from failing human and rat heart. *Proc Natl Acad Sci U S A* 2009;**106**:6854-6859.
26. Schobesberger S, Tokar S, Wright P, Bhargava A, Glukhov AV, Poulet C, Buzuk A, Monszpart A, Sikkel MB, Harding SE, Nikolaev VO, Lyon AR, Gorelik J. T-tubule remodelling disturbs localised β2-adrenergic signalling in rat ventricular myocyte during the progression of heart failure. *Cardiovasc Res* 2017; **113**: 770-782.
27. Nikolaev VO, Bunemann M, Hein L, Hannawacker A, Lohse MJ. Novel single chain cAMP sensors for receptor-induced signal propagation. *J Biol Chem* 2004;**279**:37215-37218.
28. Tulloch LB, Howie J, Wypijewski KJ, Wilson CR, Bernard WG, Shattock MJ, Fuller W. The inhibitory effect of phospholemman on the sodium pump requires its palmitoylation. *J Biol Chem* 2011;**286**:36020-36031.
29. Nikolaev VO, Bunemann M, Schmitteckert E, Lohse MJ, Engelhardt S. Cyclic AMP imaging in adult cardiac myocytes reveals far-reaching beta1-adrenergic but locally confined beta2-adrenergic receptor-mediated signaling. *Circ Res* 2006;**99**:1084-1091.
30. Xiao RP. Beta-adrenergic signaling in the heart: dual coupling of the beta2-adrenergic receptor to G(s) and G(i) proteins. *Sci STKE* 2001;**2001**:re15.
31. Juel C, Hostrup M, Bangsbo J. The effect of exercise and beta2-adrenergic stimulation on glutathionylation and function of the Na,K-ATPase in human skeletal muscle. *Physiol Rep* 2015;**3**.
32. Hostrup M, Kalsen A, Onslev J, Jessen S, Haase C, Habib S, Ortenblad N, Backer V, Bangsbo J. Mechanisms underlying enhancements in muscle force and power output during maximal cycle ergometer exercise induced by chronic beta2-adrenergic stimulation in men. *J Appl Physiol (1985)* 2015;**119**:475-486.
33. Kalsen A, Hostrup M, Backer V, Bangsbo J. Effect of formoterol, a long-acting beta2-adrenergic agonist, on muscle strength and power output, metabolism, and fatigue during maximal sprinting in men. *Am J Physiol Regul Integr Comp Physiol* 2016;**310**:R1312-1321.
34. Mehel H, Emons J, Vettel C, Wittkopper K, Seppelt D, Dewenter M, Lutz S, Sossalla S, Maier LS, Lechene P, Leroy J, Lefebvre F, Varin A, Eschenhagen T, Nattel S, Dobrev D, Zimmermann WH, Nikolaev VO, Vandecasteele G, Fischmeister R, El-

Armouche A. Phosphodiesterase-2 Is up-regulated in human failing hearts and blunts beta-adrenergic responses in cardiomyocytes. *J Am Coll Cardiol* 2013;**62**:1596-1606.

35. Kuhn M. Structure, regulation, and function of mammalian membrane guanylyl cyclase receptors, with a focus on guanylyl cyclase-A. *Circ Res* 2003;**93**:700-709.

Figure legends

Figure 1. Generation of a targeted PLM-Epac1 biosensor. (**A**) Schematic representation of the PLM-Epac1 sensor construct that includes full-length phospholemman (PLM) fused via a flexible linker to the parential cytosolic cAMP biosensor Epac1-camps comprised of the cAMP-binding domain sandwiched between enhanced yellow (YFP) and enhanced cyan (CFP) fluorescent proteins. (**B**) Representative confocal images of adult rat ventricular myocytes (ARVMs) transduced with adenoviral constructs to express Epac1-camps or PLM-Epac1. Fluorescence in YFP and CFP channels reveals striated membrane localization pattern for PLM-Epac1, as compared to the cytosolic Epac1-camps. TM, transmission image. (**C**) Representative FRET recording (n=10) of a PLM-Epac1 expressing ARVM stimulated with the β-adrenergic agonist isoproterenol (ISO, 100 nmol/L). Left, YFP and CFP intensities measured in a red-marked membrane region of interest to exclude strongly fluorescent perinuclear overexpression show concomitant changes, indicative of a decreasing YFP/CFP FRET ratio (here normalized to the basal ratio values) which represents an increase of local cAMP levels upon ISO treatment. In contrast, no detectable FRET change could be observed in perinuclear location (marked black) with sensor overexpression (right). Scale bars, 10 µm.

Figure 2. Strong local β_2-AR/cAMP signals in the PLM/NKA microdomain. (**A,B**) Representative FRET traces for Epac1-camps and PLM-Epac1 expressing ARVMs upon β_1-AR-selective stimulation (100 nmol/L ISO plus 50 nmol/L of the β_2-AR blocker ICI118551). (**C,D**) Representative FRET traces for β_2-AR-selective stimulation (100 nmol/L ISO plus 100 nmol/L of the β_1-AR blocker CGP20712A). Maximal stimulation of cAMP was subsequently achieved by the PDE2 selective inhibitor (BAY 60-7550, 100 nmol/L used in C and D, see Figure 4), the unselective PDE inhibitor IBMX (100 µmol/L) and the adenylyl cyclase activator forskolin (10 µmol/L). (**E**) Quantification of FRET responses to selective β_1- and β_2-AR stimulations shown in A-D. Number of cells (n) and hearts (N) per condition were as follows -

n/N=40/6 and n/N=33/6 for β_1-AR and n/N=31/9 and n/N=38/8 for β_2-AR, respectively. * — significant difference, P<0.05 by mixed ANOVA followed by Wald χ^2-test.

Figure 3. PDE contributions to cAMP hydrolysis under basal conditions. Representative FRET traces recorded in ARVMs expressing either cytosolic **(A**) or NKA/PLM microdomain specific (**B**) biosensor upon PDE2 inhibition with 100 nmol/L BAY 60-7550, followed by 100 µmol/L of the unselective PDE inhibitor IBMX and by 100 nmol/L ISO and 10 µmol/L forskolin to achieve maximal stimulation. (**C**) Quantification of the FRET ratio change induced by the specific PDE inhibitors (10 µmol/L cilostamide for PDE3 and 10 µmol/L rolipram for PDE4 were used, respectively) related to the maximum stimulation uncovered PDE2 as the PDE family crucial for confining the PLM/NKA compartment from the bulk cytosol at basal state. Means ± SE, number of cells (n) and hearts (N) per condition were as follows - n/N=10/4 and n/N=10/4 for PDE2, n/N=12/4 and n/N=24/6 for PDE3, and n/N=12/5 and n/N=12/5 for PDE4, respectively. * — significant differences, P<0.05 by Mann-Whitney test. n.s. - not significant, P>0.05 by mixed ANOVA followed by Wald χ^2-test.

Figure 4. PDE regulation of cytosolic and local cAMP levels under subtype specific β-AR stimulations. Representative FRET ratio traces for Epac1-camps (**A**) and PLM-Epac1 (**B**) expressing ARVMs recorded during selective β_2-AR stimulation with 100 nmol/L ISO plus 50 nmol/L CGP20712A followed by the PDE3 inhibitor cilostamide (Cilo, 10 µmol/L) and the unselective PDE inhibitor IBMX (100 µmol/L). Forskolin (10 µmol/L) was used to fully stimulate the sensors. (**C**) Quantification of the PDE inhibitor responses in cells with prestimulated β_1-AR. 100 nmol/L BAY 60-7550 and 10 µmol/L rolipram were used to inhibit PDE2 and PDE4, respectively. Shown are means ± SE, number of cells (n) and hearts (N) per condition were as follows - n/N=13/4 and n/N=14/5 for PDE2, n/N=13/4 and n/N=16/5 for PDE3, and n/N=19/3 and n/N=15/9 for PDE4, respectively. (**D**) Quantification of the PDE inhibitor responses in cells with prestimulated β_2-AR. Means ± SE, number of cells (n) and hearts (N) per condition were as follows - n/N=12/4 and n/N=13/4 for PDE2, n/N=11/4 and

n/N=16/4 for PDE3, and n/N=13/4 and n/N=14/4 for PDE4, respectively. * — significant differences, P<0.05 by mixed ANOVA followed by Wald χ^2-test. n.s. - not significant, P>0.05 by the same test.

Figure 5. Changes in local cAMP dynamics at PLM in heart failure. (A-D) Representative FRET traces for ARVMs isolated from either age-matched controls (AMC) or from rats with chronic heart failure 16 weeks after MI and transduced to express PLM-Epac1 sensor. Cells were first stimulated with 100 nmol/L ISO plus 100 nmol/L CGP20712A to activate β_2-AR followed by the PDE2 and PDE3 inhibitors and forskolin. (**E**) β_2-AR stimulation shows a significantly attenuated cAMP response in the microdmain, indicating a loss of β_2-AR/cAMP compartmentation. Data from cells expressing the cytosolic sensor Epac1-camps are also provided for comparison. Shown are means ± SE, number of cells (n) and hearts (N) per condition were as follows - n/N=27/4 and n/N=26/4 for AMC, and n/N=23/4 and n/N=27/4 for MI groups, respectively. (**F**) Data analysis for the experiments shown in A-D. In heart failure, there is a pronounced increase in local PDE2 and a decrease in local PDE3 inhibitor effects. Compound concentrations were as in Figure 4. Means±SE, number of cells (n) and hearts (N) per condition were as follows - n/N=7/4 and n/N=6/3 for PDE2, and n/N=12/4 and n/N=9/3 for PDE3, respectively. * — significant differences, P<0.05 by mixed ANOVA followed by Wald χ^2-test.

Figure 6. Immunoblot analysis of PLM phosphorylation. (A) Representative immunoblots for ARVMs isolated from either controls (AMC) or from rats with chronic heart failure after MI. Cells were stimulated for 5 min with 100 nmol/L ISO plus 100 nmol/L CGP20712A to selectively activate β_2-AR. PLM phosphorylation was analyzed using a Ser68 phosphoantibody. In healthy cells, β_2-AR stimulates PLM phosphorylation, this effect is blunted in heart failure. Data analysis is in (**B**). Means±SE, number of blots/hearts were 6/3 and 5/3 for control and stimulated groups, respectively. * — significant difference, P<0.05 by one-way ANOVA.

Figure 7. Schematics depicting local regulation of cAMP in the NKA/PLM microdomain and its changes in heart failure. In healthy ARVMs, NKA/PLM is in close functional proximity to the β_2-AR and PDE3. In disease, receptor and PDE redistribution disrupts the proper β_2-AR signaling to cAMP/PKA/PLM. Local increase of PDE2 mediated effects and a decrease of PDE3 co-localization with the microdomain can be detected in disease.

Figure 1 (Bastug-Özel et al.)

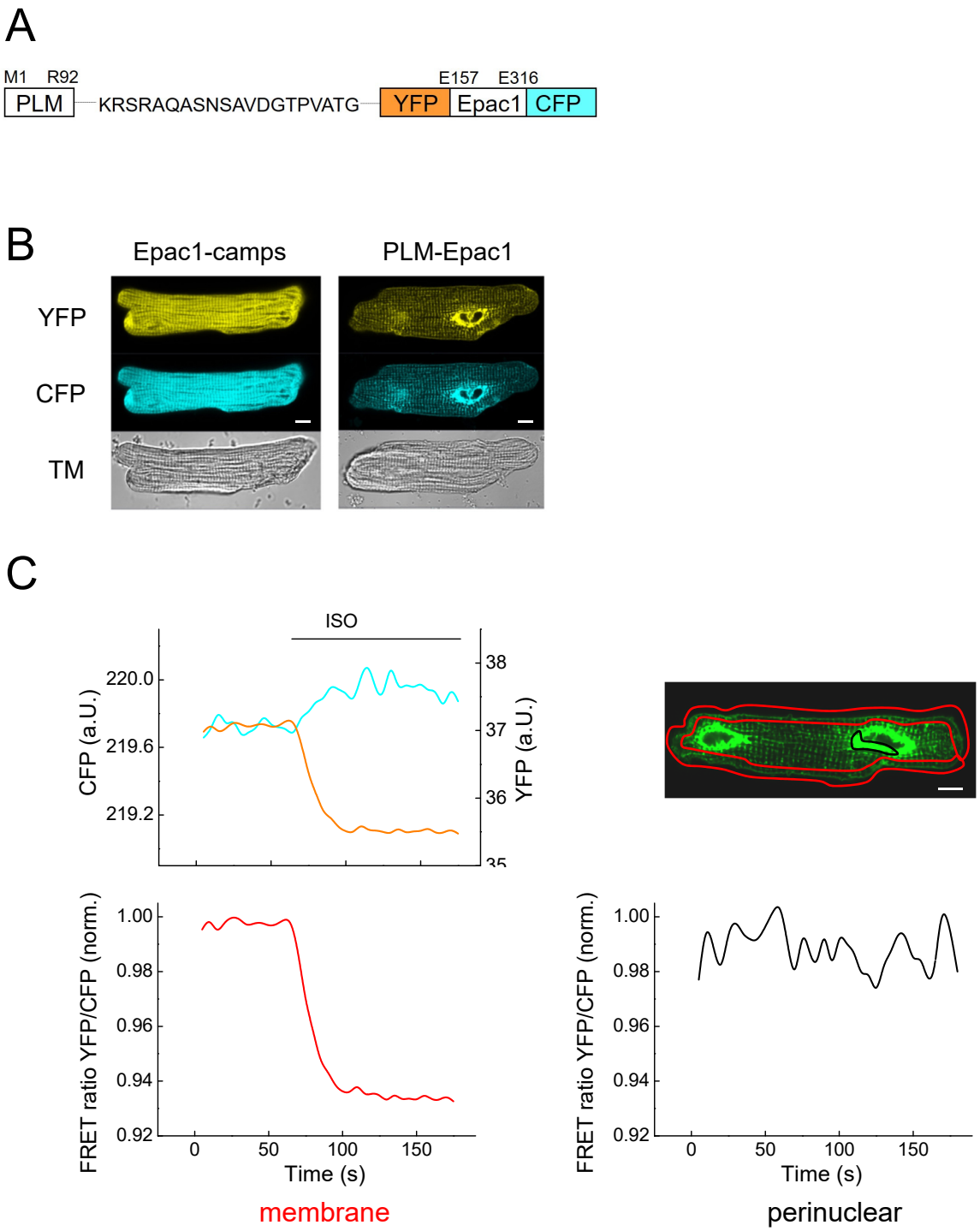


Figure 2 (Bastug-Özel et al.)

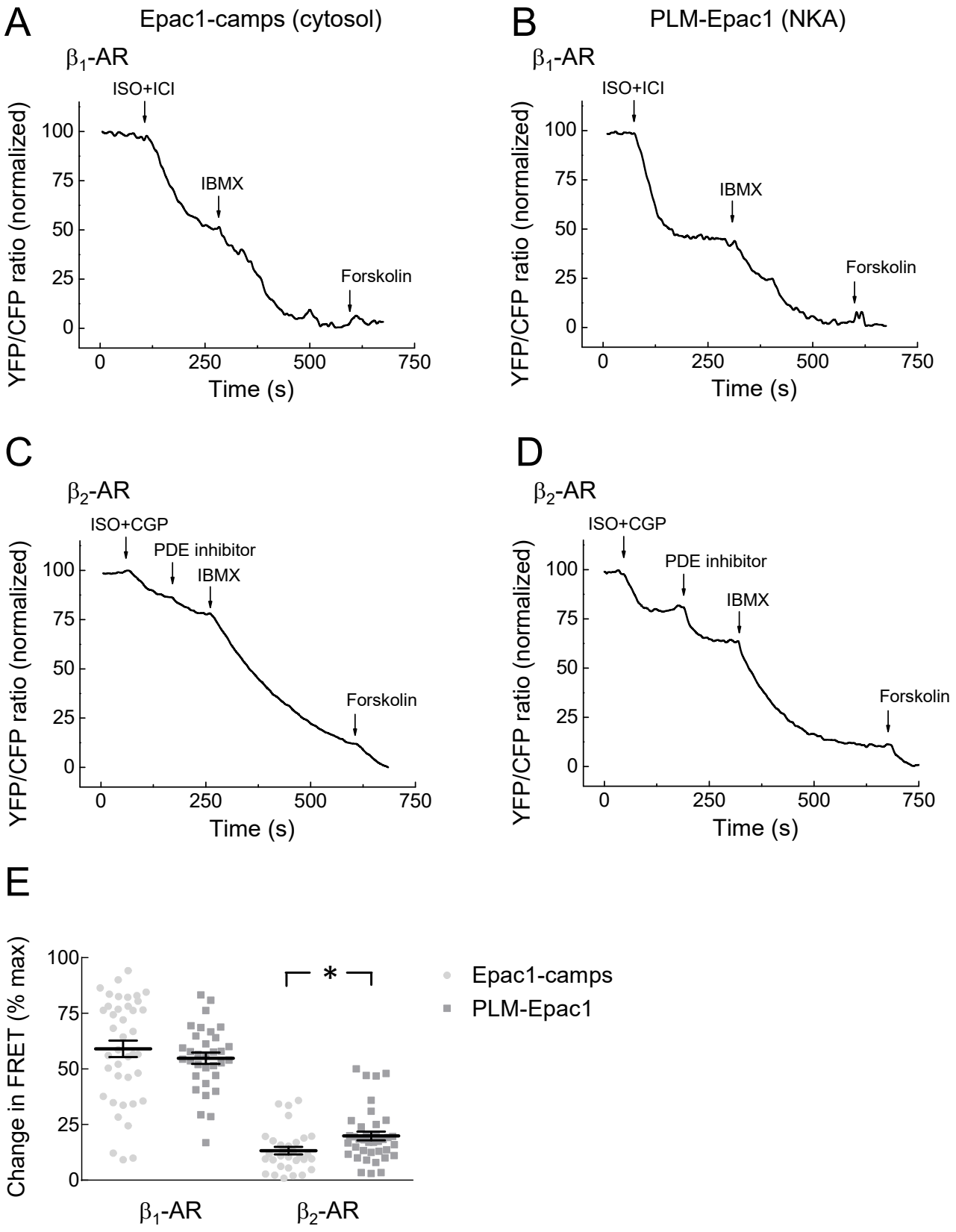


Figure 3 (Bastug-Özel et al.)

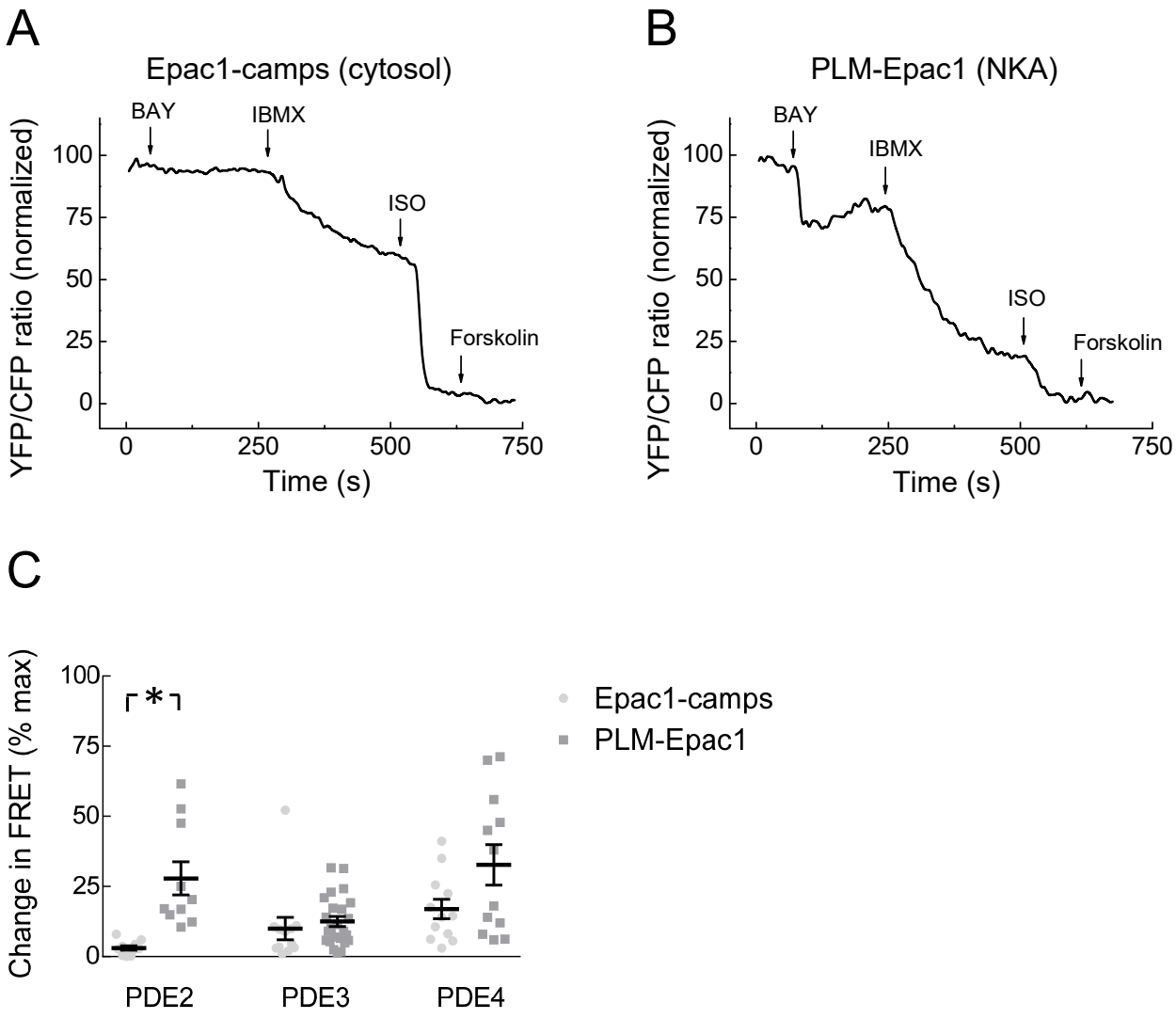


Figure 4 (Bastug-Özel et al.)

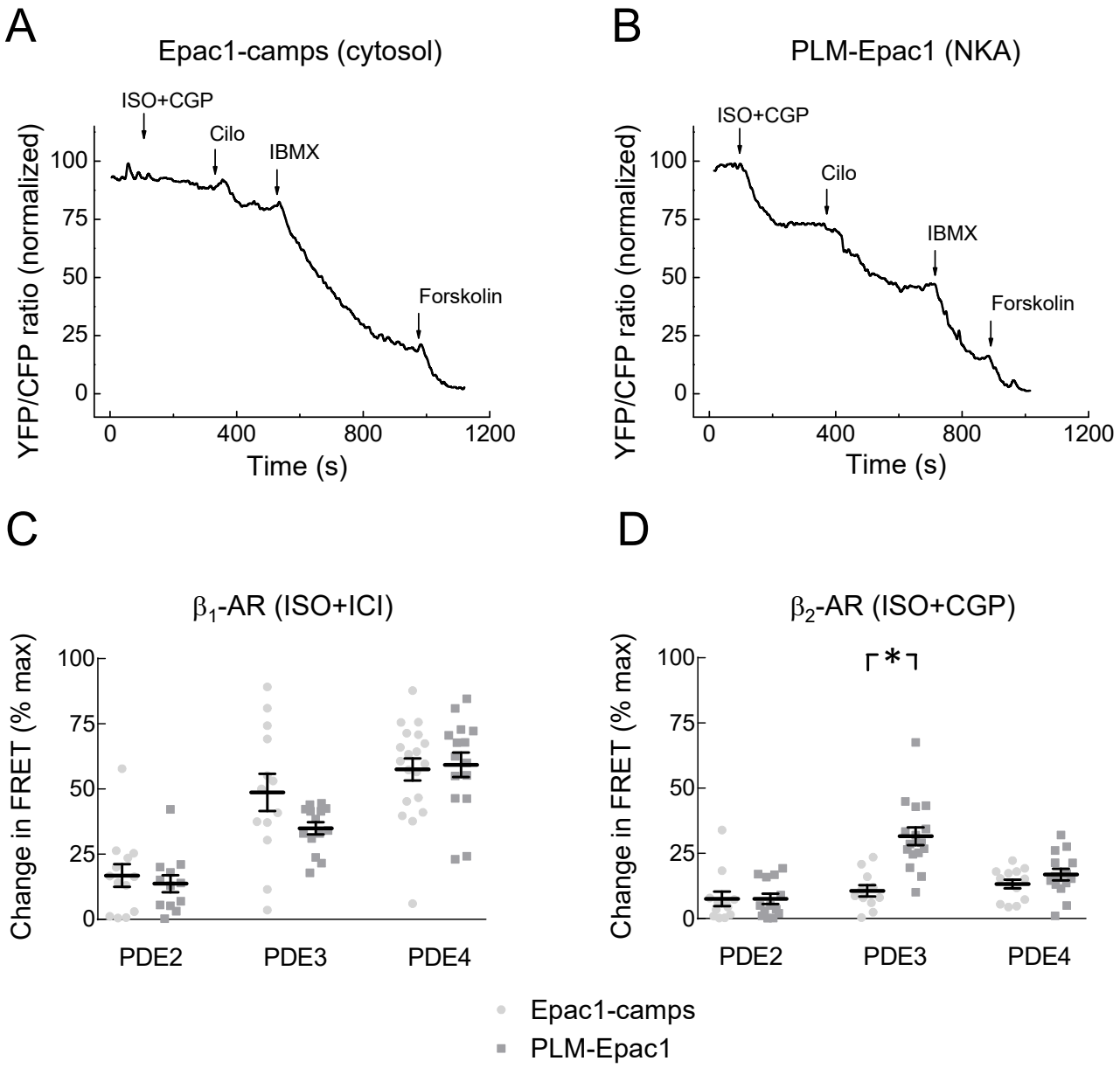


Figure 5 (Bastug-Özel et al.)

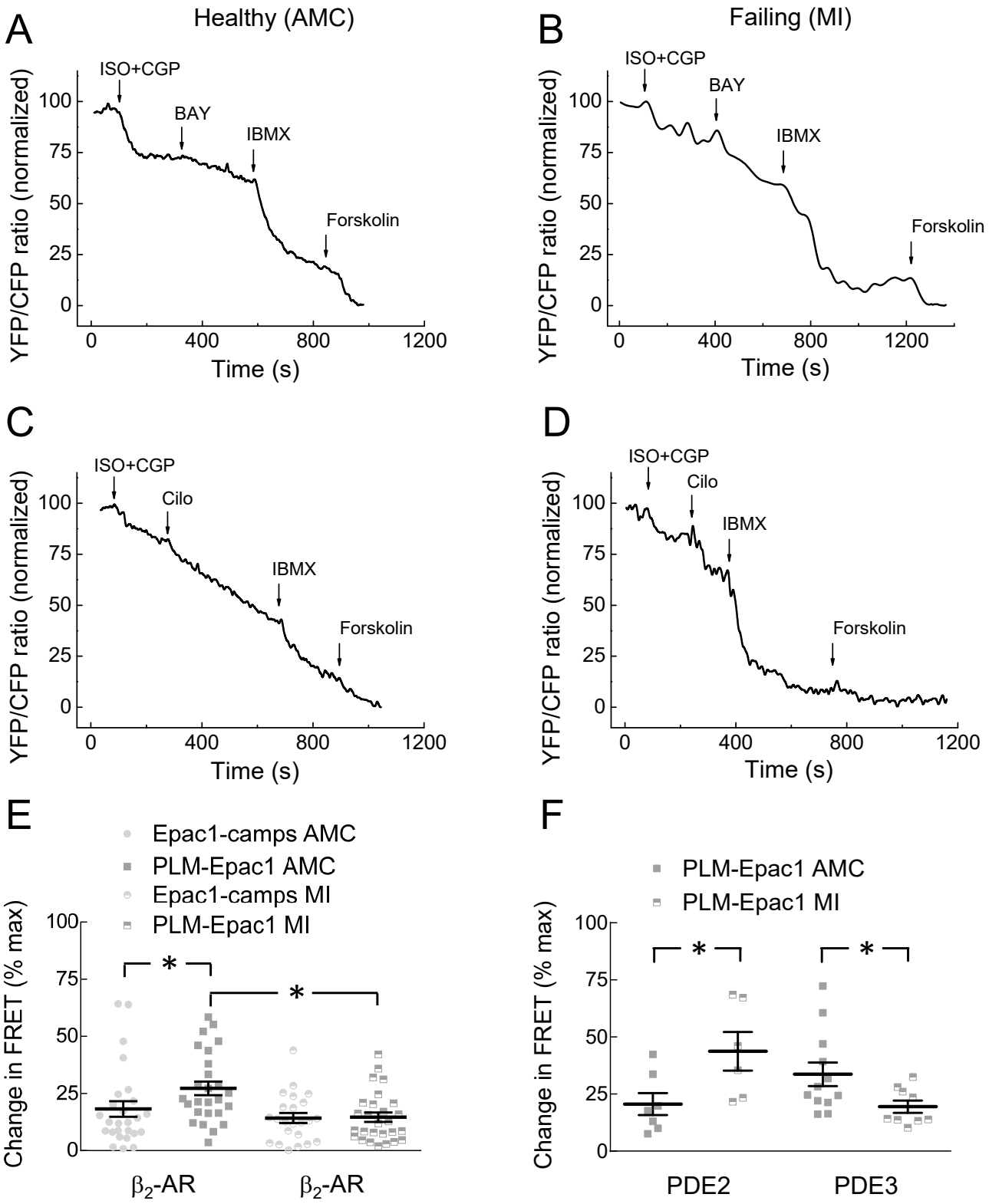
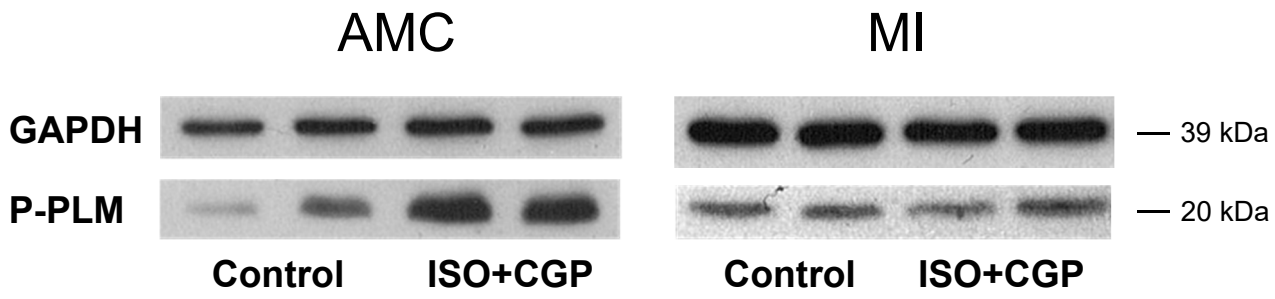


Figure 6 (Bastug-Özel et al.)

A



B

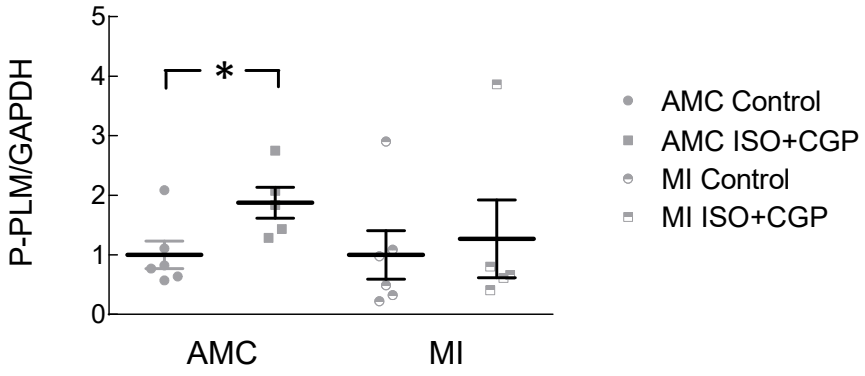
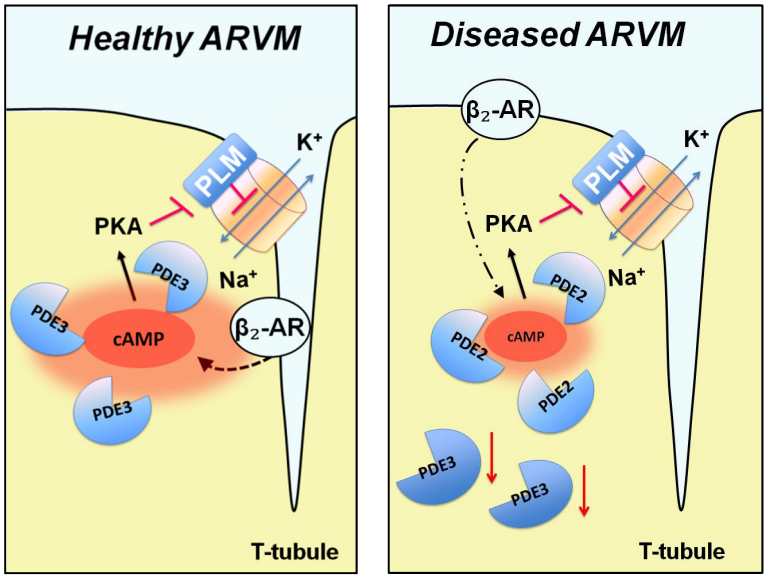
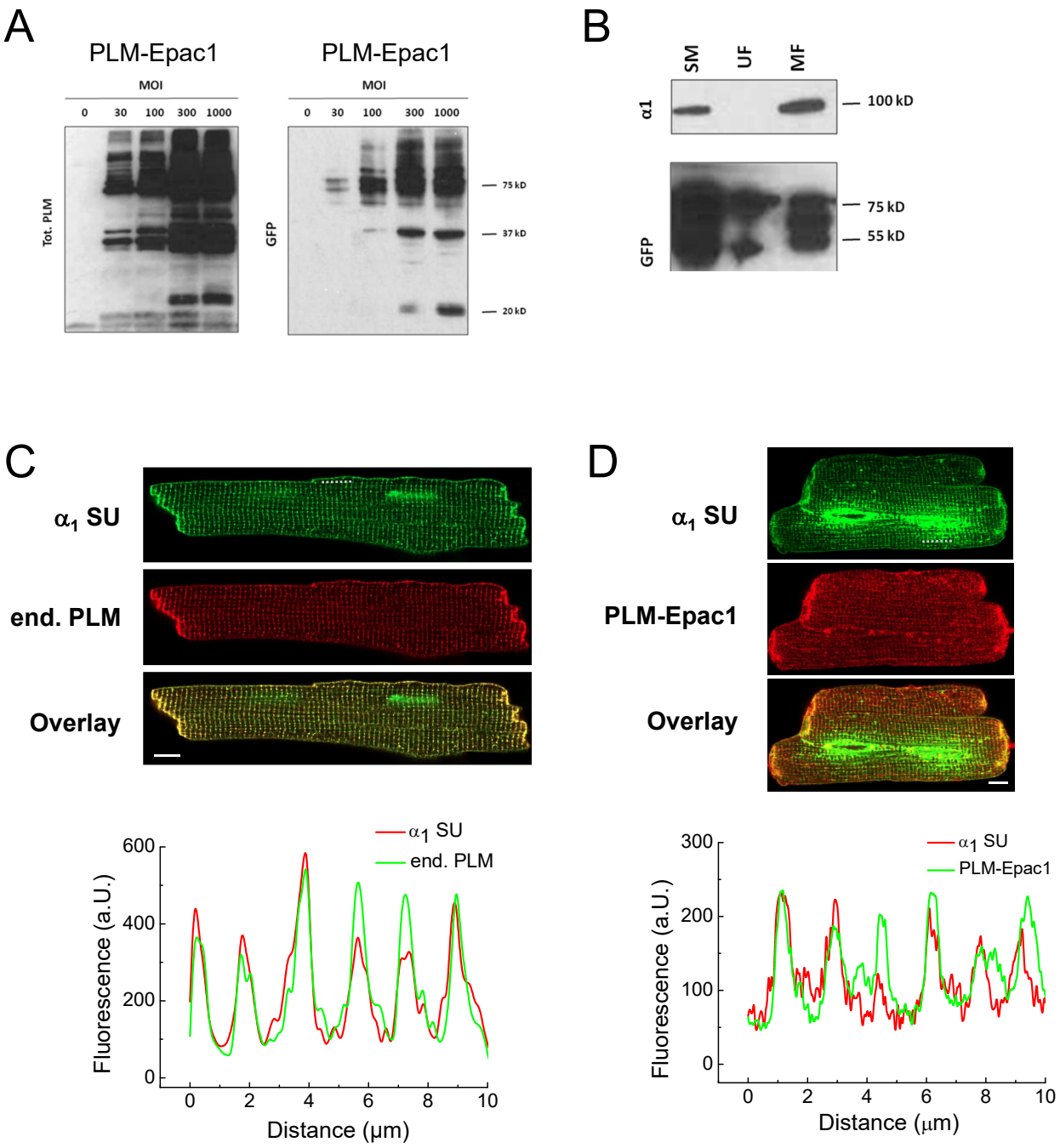


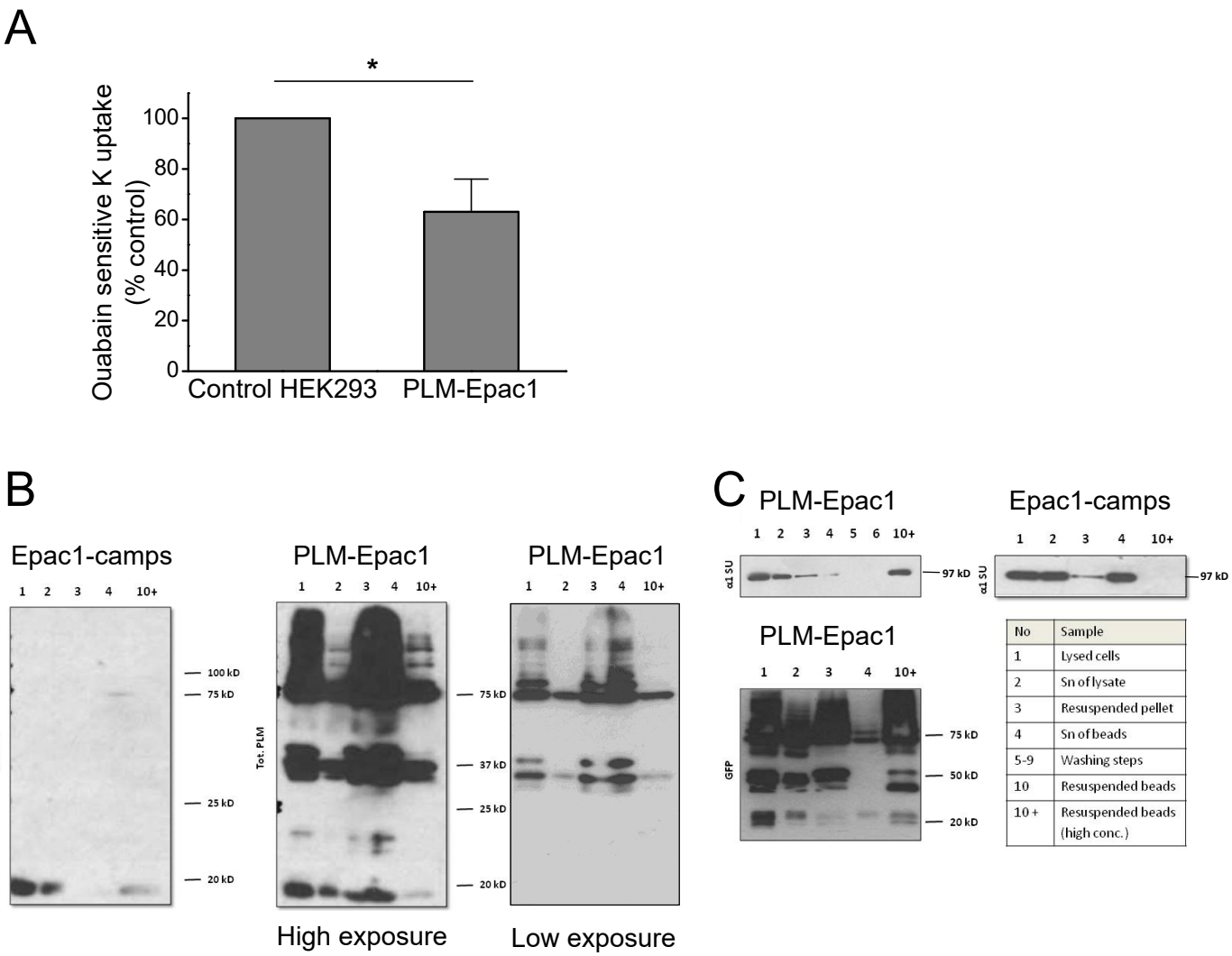
Figure 7 (Bastug-Özel et al.)



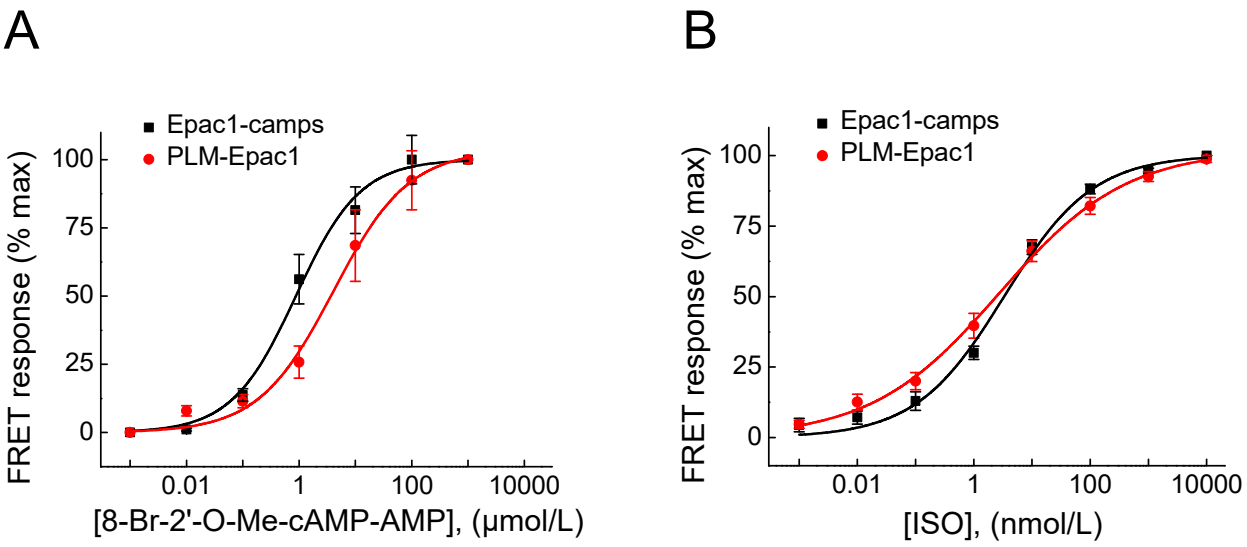
Click here to download Supplementary Material - Other PLM Paper Suppl Figures CVR revised.pdf



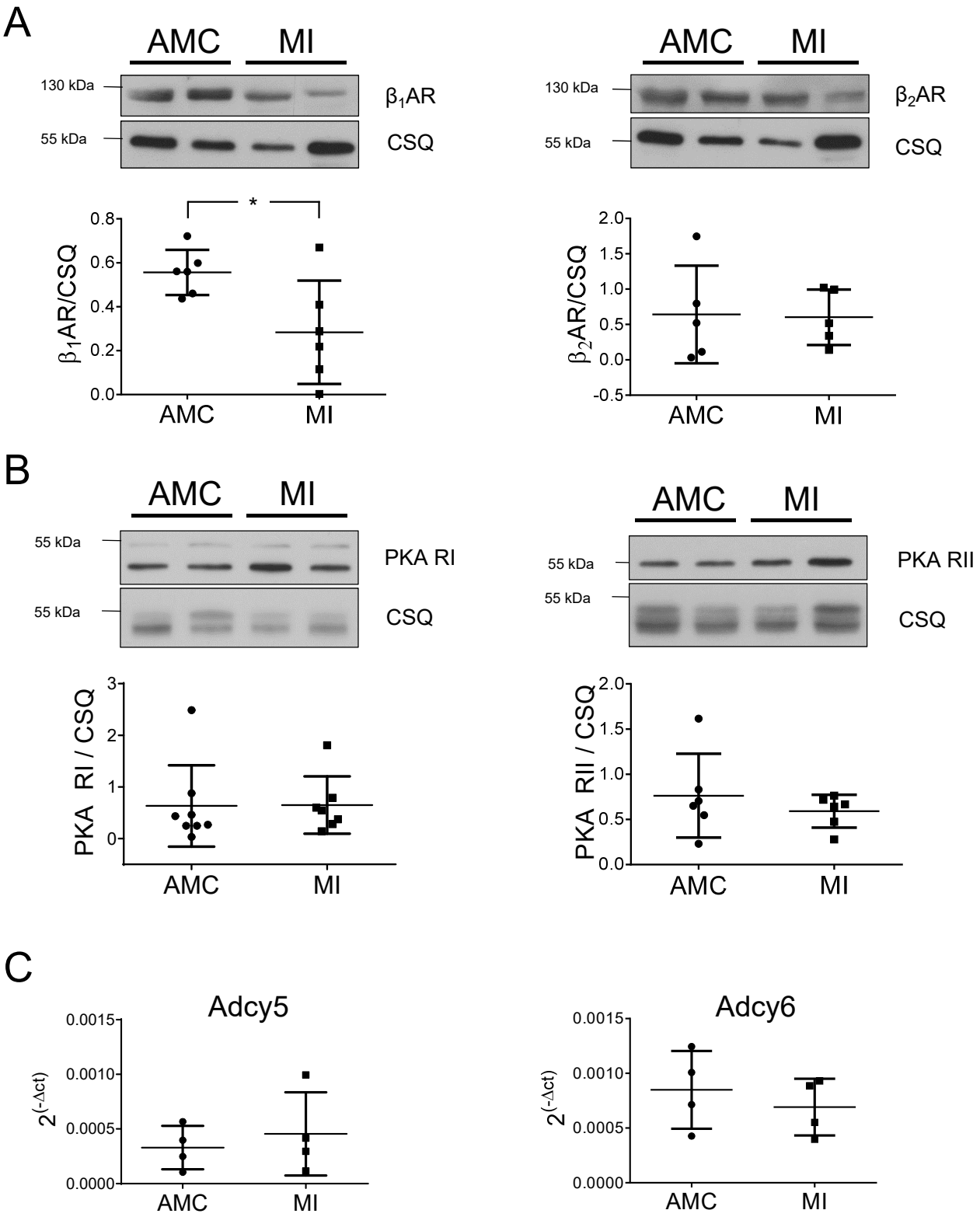
Supplementary Figure 1. Expression and co-localization of PLM-Epac1 with the NKA α_1 subunit. (**A**) Immunoblot analysis for the adenoviral expression of PLM-Epac1 in ARVMs at the multiplicity of infection (MOI) of 10, 30, 100, 300 or 1000. Cell lysates were subjected to 10 % SDS-PAGE and immunoblotting using anti-PLM and anti-GFP antibodies (which detects CFP and YFP moieties of the biosensor). Blots showing PLM-Epac1 at ~ 75 kD are representative of at least three individual experiments. (**B**) Representative immunoblot (n=3) showing cell surface biotinylation of PLM-Epac1 transduced ARVMs. Biotinylated cell surface proteins that were not degraded during lysis (Starting Material, SM) were purified using streptavidin-sepharose beads. Collected unbound fraction (UF) and cell surface proteins in the membrane fraction (MF) were immunoblotted for PLM-Epac1 using anti-GFP and anti-NKA α_1-subunit antibodies. (**C,D**) Representative confocal images (n=7 each) of untransduced and PLM-Epac1 transduced (MOI 300) ARVMs immunostained for co-localization of PLM with NKA α_1-subunit (α_1 SU) confirmed by the intensity overlay of both fluorescent signals. end. PLM, endogenous PLM. Scale bars, 10 μm.



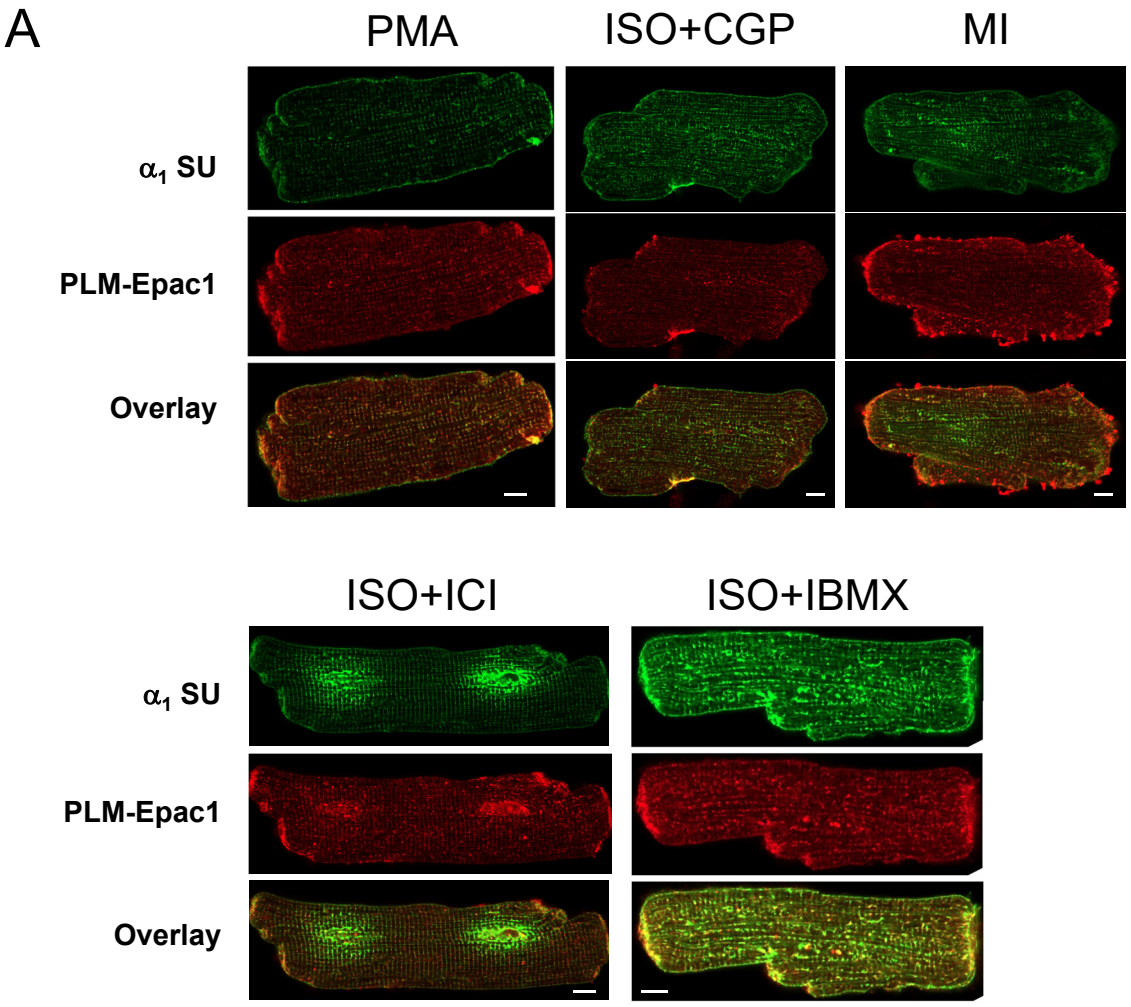
Supplementary Figure 2. Functionality and physical association of PLM-Epac1 with the sodium-potassium pump. (**A**) Quantification of PLM-Epac1 mediated inhibition of NKA activity. Sodium pump activity was measured as ouabain-sensitive ^{86}Rb uptake in HEK293 cells stably expressing PLM-Epac1. In this assay, pump activity is expressed as a percentage of the activity measured in untransfected HEK293 cells which do not express PLM. Means ± SE, n=8 from 3 independent assays, *—significant differences, $P<0.05$ by one-way ANOVA. (**B**) ARVMs were transduced with PLM-Epac1 or Epac1-camps (negative control), immunoprecipitatied using anti-NKA α_1-subunit monoclonal antibody preimmobilized on protein G-sepharose beads and immunobloted for total PLM. Shown are representative immunoblots (n=3) for various samples numbered as described in the table (see C, right). Both the sensor PLM-Epac1 (~75 kD) and the endogenous PLM (~17 kD) are pulled down using this antibody. (**C**) Representative immunoblots for co-immunoprecipitation experiments (n=3) with PLM-Epac1 and Epac1-camps precipitated using GFP-Trap® under identical conditions as in B and immunoblotted for NKA α_1-subunit or GFP as shown. All blots are representatives for at least three individual experiments.

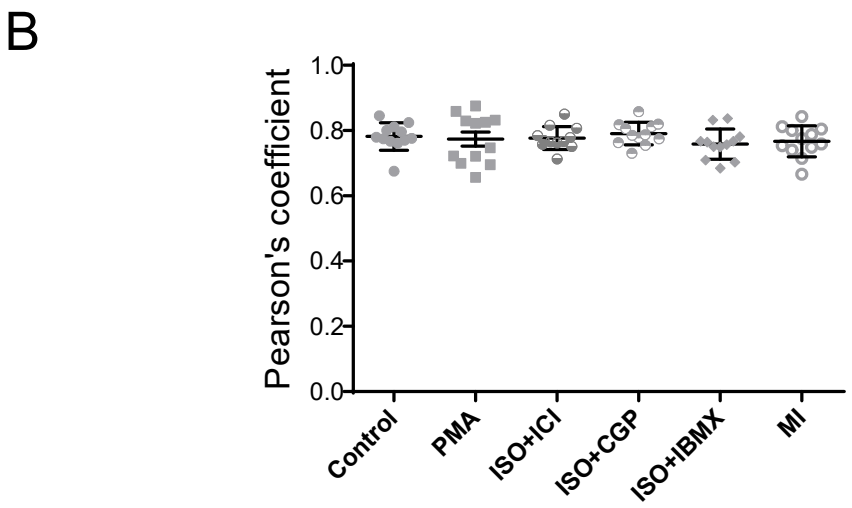


Supplementary Figure 3. Sensitivity of Epac1-camps and PLM-Epac1. (**A**) Concentration response dependencies measured in PLM-Epac1 and Epac1-camps transduced ARVMs pretreated with the adenylyl cyclase inhibitor MDL12,330A (100 µmol/L) for 10 minutes and stimulated with increasing concentrations of the cell-permeable cAMP analogue cAMP 8-Br-2'-O-Me-cAMP-AM. This analogue can be used for direct in cell sensor calibration since it has the same affinity for the sensor binding domains as native cAMP (see Ref. 23). PLM-Epac1 shows a slightly lower affinity than the cytosolic Epac1-camps sensor. EC_{50} values were 4.1±1.1 and 0.9±0.2 µmol/L, respectively. Means±SE, n=7 and 12 cells from 4 and 5 rat hearts, respectively. (**B)** FRET responses to increasing ISO concentrations in Epac1-camps and PLM-Epac1 expressing ARVMs show no significant differences in terms of ISO potency. EC_{50} values were 4.4±1.2 and 4.3±0.7 nmol/L, respectively. Means±SE, n=15 and 10 cells from 4 rat hearts each.

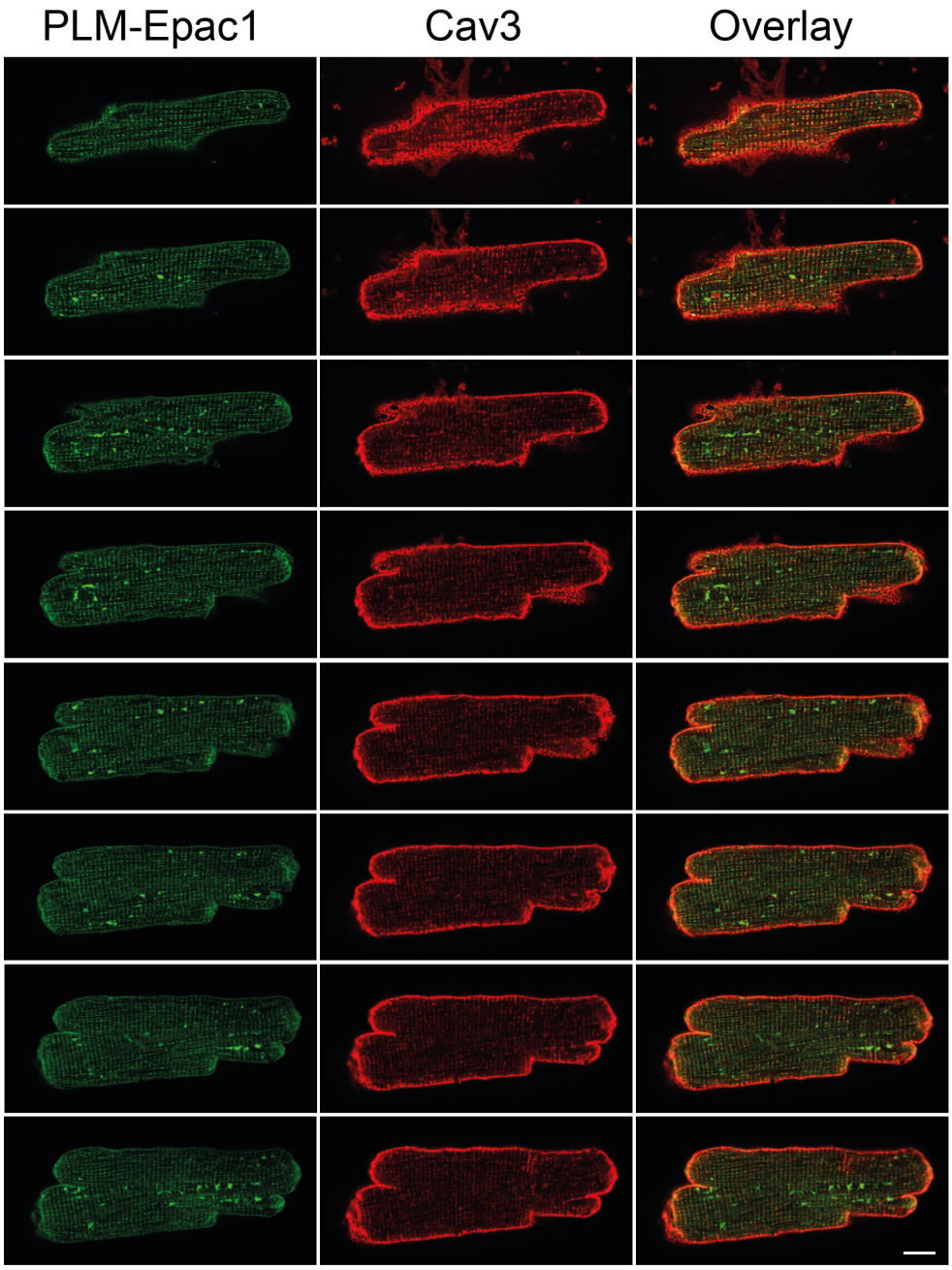


Supplementary Figure 4. qPCR and immunoblot analysis for crucial components of the β-adrenergic/cAMP pathway in healthy (AMC) and failing (MI) myocytes. (A) ARVMs lysates were immunoblotted for b1- (n=6) and b2-AR (n=5). (B) Levels of pKA regulatory subunits RI (n=8) and RII (n=6 each) were quantified by immunoblot. (C) qPCR results for the major cardiomyocyte adenylyl cyclase families AC5 (Adcy5) and AC6 (Adcy6), n=4 each. * - significant difference ($p<0.05$) by one-way ANOVA. All other differences are not significant at $p=0.05$ by the same test.

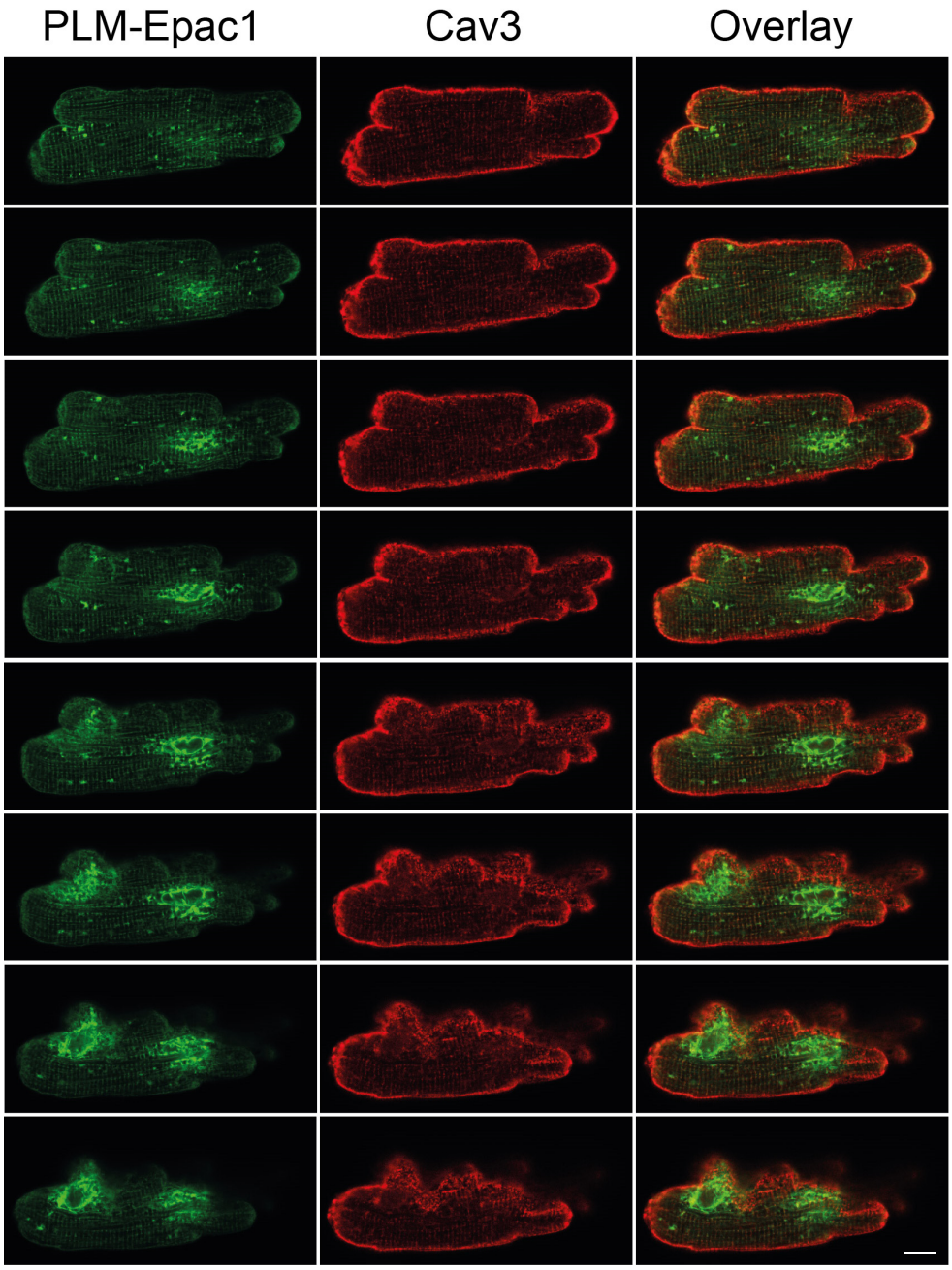




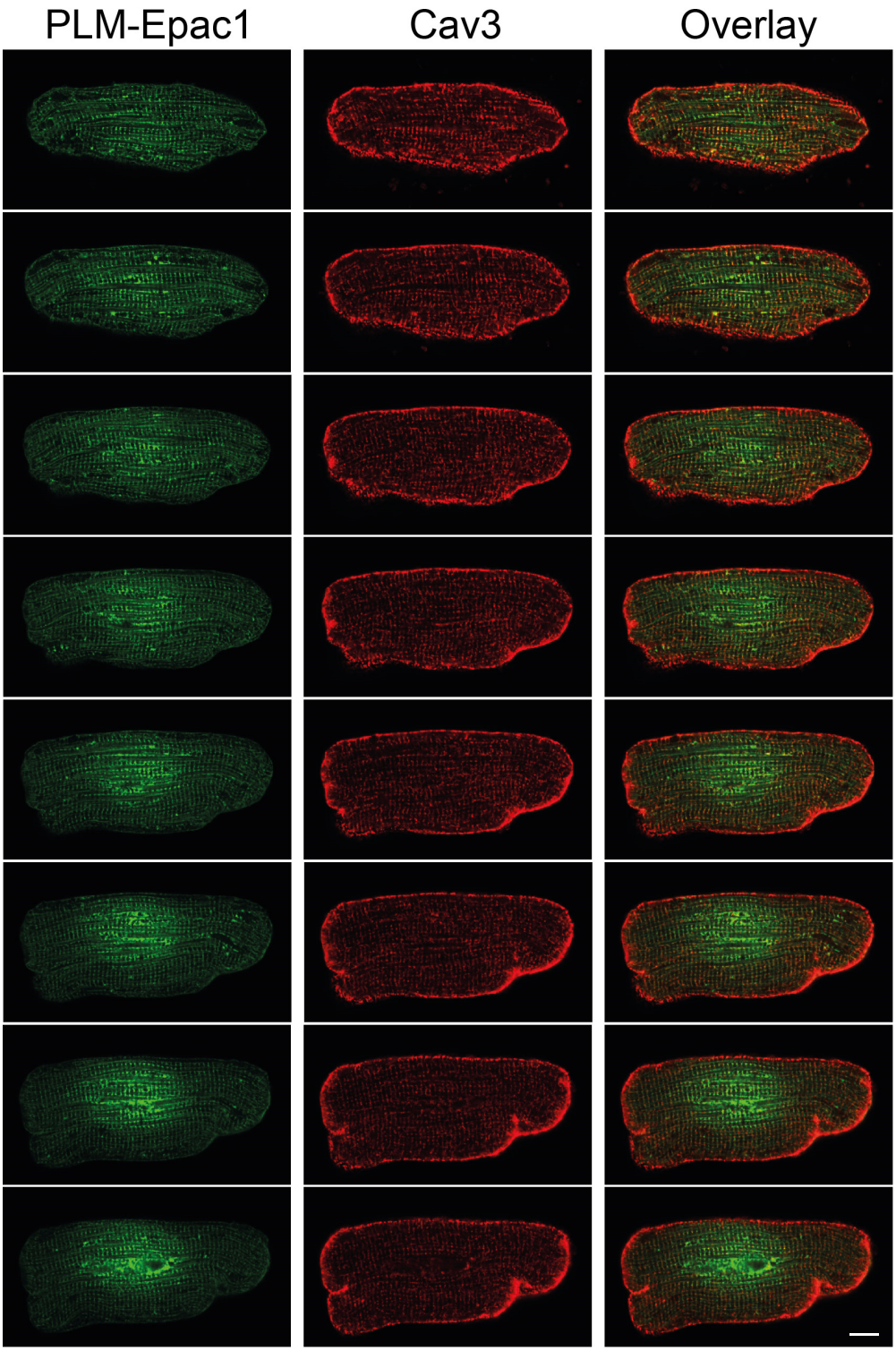
Supplementary Figure 5. Co-localization of PLM-Epac1 with NKA under various conditions. (A) Representative confocal images of PLM-Epac1 transduced (MOI 300) healthy or failing (MI) ARVMs. Healthy cells were stimulated for 5 min with 10 µmol/L phorbol 12-myristate 13-acetate (PMA), β_2-AR ligands (100 nmol/L ISO plus 100 nmol/L CGP20712A=CGP), β_1-AR ligands (100 nmol/L ISO plus 50 nmol/L ICI118551=ICI) or with ISO in combination with a broadband PDE inhibitor (IBMX, 100 µmol/L), fixed with 4% PFA and immunostained for NKA α1-subunit (α1 SU). Scale bars, 10 µm. Example of an unstimulated healthy cell is in Supplementary Figure 1D. (B) Quantification of the data from A using Pearson's co-localization coefficient (N/n=3/12 each) shows no significant differences between unstimulated and any stimulated groups, by mixed ANOVA followed by Wald χ^2-test.



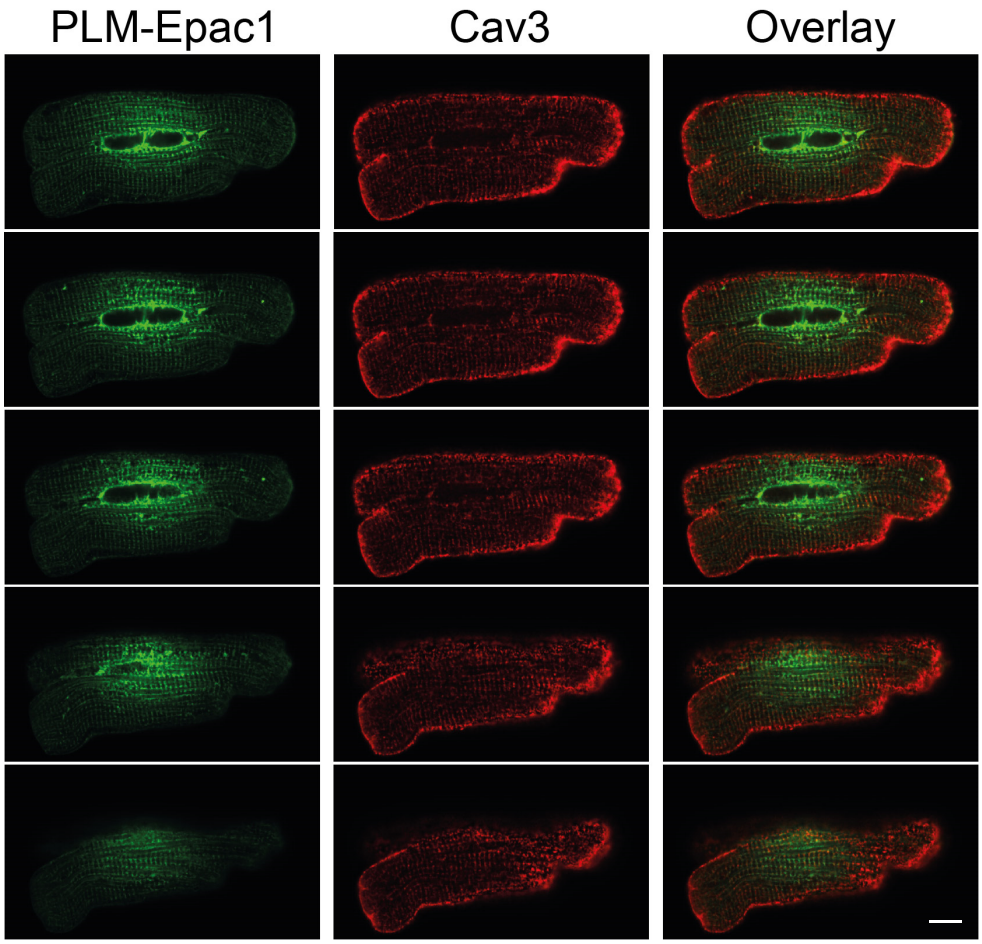
Supplementary Figure 6. Confocal microscopy analysis of PLM-Epac1 transfected healthy cardiomyocytes stained with caveolin 3 antibody. Representative z-stack images (1.5 µm steps from bottom/glass surface to the top) acquired for cells isoated from AMC animals (N/n=3/10). Scale bar, 15 µm.



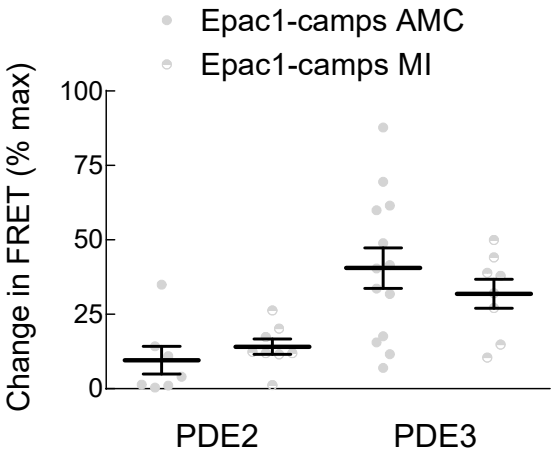
Supplementary Figure 6 (continued). Confocal microscopy analysis of PLM-Epac1 transfected healthy cardiomyocytes stained with caveolin 3 antibody. Representative z-stack images (1.5 µm steps from bottom/glass surface to the top) acquired for cells isoated from AMC animals (N/n=3/10). Scale bar, 15 µm.



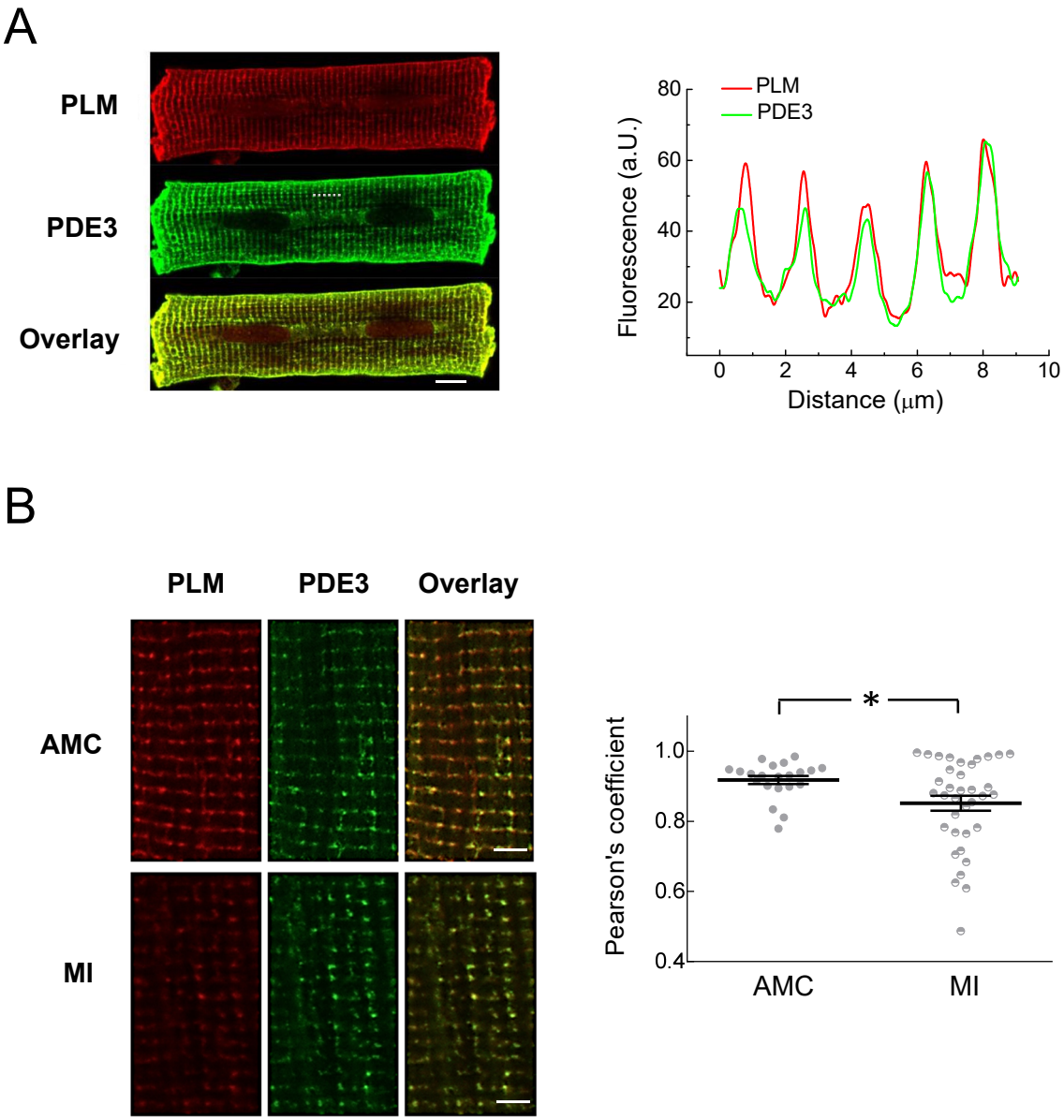
Supplementary Figure 7. Confocal microscopy analysis of PLM-Epac1 transfected failing cardiomyocytes stained with caveolin 3 antibody. Representative z-stack images (1.5 µm steps from bottom/glass surface to the top) acquired for MI cells (N/n=3/10). Scale bar, 15 µm.



Supplementary Figure 7 (continued). Confocal microscopy analysis of PLM-Epac1 transfected failing cardiomyocytes stained with caveolin 3 antibody. Representative z-stack images (1.5 µm steps from bottom/glass surface to the top) acquired for MI cells (N/n=3/10). Scale bar, 15 µm.



Supplementary Figure 8. Effects of PDE2 and PDE3 inhibitors on cytosolic cAMP after β_2-AR stimulation in healthy and failing myocytes. Cells were prestimulated with 100 nmol/L ISO plus 100 nmol/L CGP20712A, after which 100 nmol/L BAY 60-7550 for PDE2 and 10 µmol/L cilostamide for PDE3 were applied as described in Figure 5A-D. Data analysis shows no significant differences for PDE2 and PDE3 inhibitor effects measured by Epac1-camps between healthy and failing cells. Means ± SE, number of cells (n) and hearts (N) were as follows - N/n=3/7, N/n=3/8 for PDE2 and N/n=3/13, N/n=3/8 for PDE3. There are no significant differences between AMC and MI groups by mixed ANOVA followed by Wald χ^2-test.



Supplementary Figure 9. Confocal microscopy analysis of PDE3A/PLM co-localization. (**A**) Representative confocal image (n=10) of a healthy ARVM immunostained with specific anti-PLM and anti-PDE3A antibodies showing a high degree of co-localization by the intensity overlay of both fluorescent signals. Scale bar, 10 μm. (**B**) Representative confocal images of age-matched control (AMC) and MI cells immunostained under the same conditions. Scale bar, 5 μm. Significant decrease of co-localization between PLM and PDE3 in diseased cells as calculated using Pearson's co-localization coefficient. Means ± SE, number of cells (n) and hearts (N) was N/n=3/21, N/n=3/36 for AMC and MI, respectively. * — significant differences, P<0.05 by Mann-Whitney test.